

AdRGD-IL12 and Ad-IL12 was 10^9 VP/tumor. This dose provided an anti-tumor effect but did not cause a decrease in body weight.

3.3. Mechanism underlying the improved anti-tumor effects of AdRGD-IL12 application

In order to analyze the mechanism underlying the enhanced anti-B16BL6 tumor effects upon intratumoral injection of AdRGD-IL12, we compared the cytolytic activities of NK cells and B16BL6-specific CTLs in mice injected with AdRGD-IL12 or Ad-IL12 at 10^9 VP/tumor. One week after Ad-treatment, the splenocytes were prepared and directly used in the Eu-release assay for NK-sensitive YAC-1 cells. On the other hand, the surplus of splenocytes was in vitro restimulated for 5 days with inactivated B16BL6 cells, which were pretreated with IFN- γ to promote the expression of their major histocompatibility complex class I molecules, for CTL expansion. As shown in Fig. 3A, the splenic NK activity was augmented after intratumoral injection of AdRGD-IL12 or Ad-IL12 as compared with tumor-free (intact) mice or B16BL6 tumor-bearing mice intratumorally injected with PBS, and the highest cytolytic activity was detected in the AdRGD-IL12-injected group. In vitro restimulated effector cells from the PBS-injected group revealed lower cytolytic activity than those from intact mice (Fig. 3B). This phenomenon suggested that differentiation, antigen priming, and/or activation of T cells might be suppressed in B16BL6 tumor-bearing mice. Nevertheless, intratumoral injection of Ad-IL12 could increase cytolytic activity of CTL effector against B16BL6 cells, and more

potent activity was detected in restimulated splenocytes from AdRGD-IL12-injected mice. Because no cytolytic effects against syngeneic irrelevant EL4 cells were detected in restimulated effector cells from any group (Fig. 3C), it was confirmed that cytolytic activities in Fig. 3B were caused by B16BL6-specific CTLs. Therefore, the enhancement of both nonspecific NK activity and B16BL6-specific CTL activity might improve the anti-B16BL6 melanoma response to intratumoral injection of AdRGD-IL12.

Furthermore, in order to confirm that NK cells and CTLs were the major effector cells responsible for B16BL6 tumor regression in mice intratumorally injected with AdRGD-IL12, we performed in vivo depletion analysis using specific antibodies against CD4, CD8, and asialoGM1 (Fig. 4). The depletion of CD8⁺ T cells or NK cells weakened the anti-tumor efficacy induced by intratumoral injection of AdRGD-IL12, whereas tumor growth inhibition was not affected by CD4⁺ T cell depletion. Additionally, the anti-tumor effect was more notably suppressed by depletion of three kinds of lymphocyte subsets. These results clearly demonstrated that CD8⁺ CTLs and NK cells were the predominant effector cells in anti-B16BL6 melanoma immunity induced by intratumoral injection of AdRGD-IL12.

3.4. Adverse effects in mice intratumorally injected with AdRGD-IL12 or Ad-IL12 at high dose

Gene therapy that induces locally persistent cytokine production is an attractive strategy for preventing severe adverse effects upon systemic administration of cytokines at high dose. Cytokine gene therapy represents about 20% of

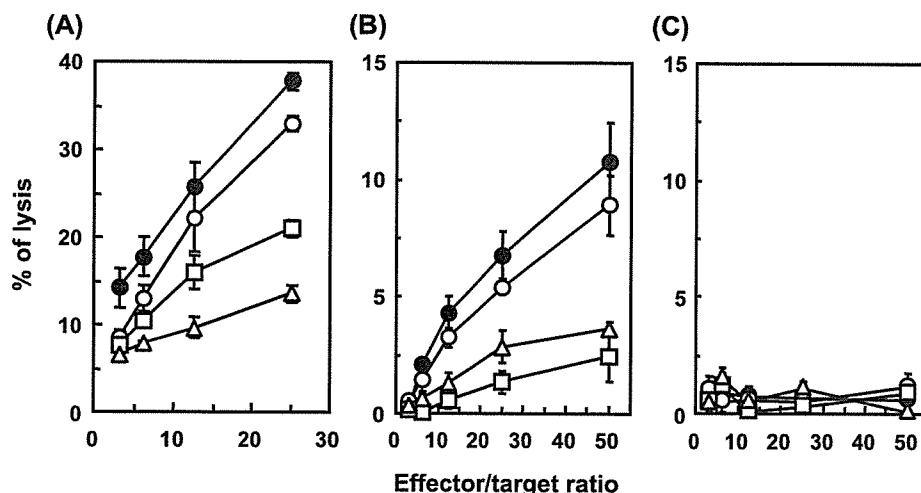


Fig. 3. NK activity and B16BL6-specific CTL activity of splenocytes from mice injected intratumorally with AdRGD-IL12 or Ad-IL12. B16BL6 cells were intradermally inoculated into C57BL/6 mice at 2×10^5 cells/mouse. Six days later, the tumors were injected with Ad-IL12 at 10^9 VP/tumor (○), AdRGD-IL12 at 10^9 VP/tumor (●), or PBS (□). At 1 week after treatment, non-adherent splenocytes were prepared from these mice. Likewise, splenocytes from tumor-free (intact) mice (△) were prepared. Splenocytes were directly used in cytolytic assays against NK-sensitive YAC-1 cells (A), or restimulated in vitro for 5 days with IFN- γ -stimulated and mitomycin C-inactivated B16BL6 cells for CTL expansion. A cytolytic assay for CTL effector was performed using B16BL6 cells (B) and syngeneic irrelevant EL4 cells (C). Cytolytic activity (% lysis) was calculated according to the formula described in Materials and methods. Each point represents the mean \pm S.E. from three independent cultures using splenocytes prepared from three individual mice.

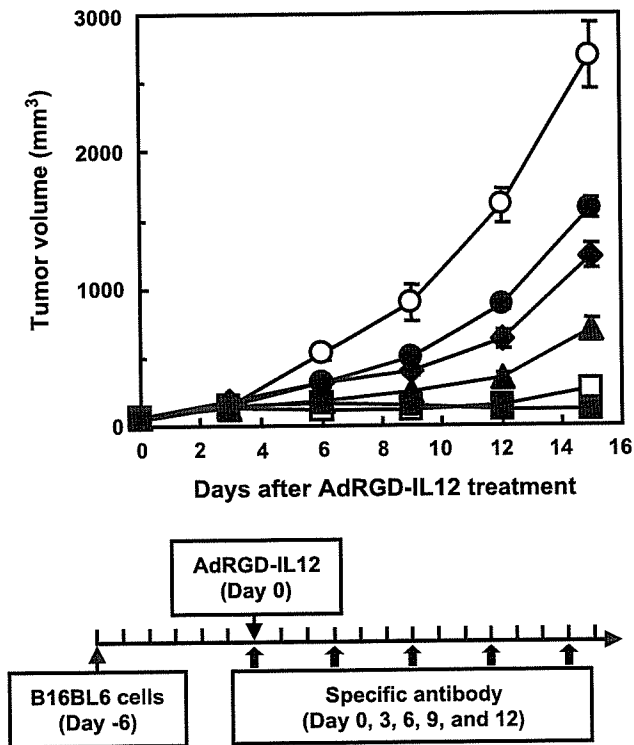


Fig. 4. Determination of immune subsets responsible for B16BL6 tumor regression induced by intratumoral administration of AdRGD-IL12. B16BL6 cells were intradermally inoculated into C57BL/6 mice at 2×10^5 cells/mouse. Six days later, the tumors were injected with AdRGD-IL12 at 10^9 VP/tumor (\square), or PBS (\circ). The antibodies GK1.5 (anti-CD4) alone (\blacksquare), 53-6.72 (anti-CD8) alone (\blacktriangle), anti-asialoGM1 alone (\blacklozenge), or combination of these three antibodies (\bullet), were intraperitoneally injected according to the indicated schedule. Depletion of T cell subsets and NK cells was monitored by flow cytometry, which showed >90% specific depletion in splenocytes at day 4 after the first antibody administration. Each point represents the mean \pm S.E. of six mice.

total clinical research protocols for gene therapy. However, we observed an extreme reduction in body weight in addition to tumor regression in mice intratumorally injected with AdRGD-IL12 or Ad-IL12 at high dose (Fig. 2). This result agrees with our previous study using AdRGD-TNF α and suggests that IL-12, which is expected to leak from the tumors into circulation, may be a cause of the adverse effects [4]. Because identification of the mechanism causing adverse effects is important for establishing the clinical protocol for in vivo cytokine gene therapy, we investigate the correlation between serum IL-12 concentrations and body weight change in mice injected intratumorally with Ad-IL12 or AdRGD-IL12 at 10^{10} or 10^{11} VP (Fig. 5A and C). Mice injected with AdRGD-IL12 or Ad-IL12 at 10^{11} VP/tumor exhibited 6–10 ng IL-12/ml serum on day 1 after Ad-treatment, which then rapidly decreased. Although the maximum body weight reduction in these mice was observed on days 5–6 after Ad-treatment, serum IL-12 concentration was 0.2 ng/ml at this time. Therefore, the rise in IL-12 concentration in the blood was not the direct cause of body weight reduction in mice treated with IL-12-expressing vector at high dose.

Because the antitumor properties of IL-12 are mediated in large part by IFN- γ , we simultaneously measured IFN- γ concentrations in sera from these mice. Despite the 20-min half-life of IFN- γ in blood, serum IFN- γ levels were dramatically elevated up to 5 days after Ad-treatment in mice treated with 10^{11} VP of each vector, and the IFN- γ profile in sera was well correlated with body weight changes in all tested groups (Fig. 5B). Serum IL-12 and IFN- γ concentrations were undetectable in mice intravenously injected with 10^{10} AdRGD-IL12 or intratumorally injected with 10^9 AdRGD-IL12 or 10^{11} AdRGD-Luc, which was the control vector expressing firefly luciferase (data not shown), and weight reduction was not observed. Additionally, TNF- α , which is known to be secreted from responder cells by IL-12 stimulation, was only detected at low levels (0.1–0.2 ng/ml) in sera from mice treated with 10^{11} VP of each vector on days 5 and 7 after Ad-treatment (data not shown). These results strongly suggested that the adverse effects observed in mice injected intratumorally with Ad-IL12 or AdRGD-IL12 at high dose were caused by a systemic inflammatory reaction triggered by high levels of endogenous IFN- γ . The secondary production of endogenous IFN- γ was induced by the leakage of IL-12 from Ad-treated B16BL6 tumors. Therefore, to ensure the safety of in vivo cytokine gene therapy using AdRGD for melanoma, we must avoid protocols that include high-levels of cytokines, which leak into the circulating blood from the tumor.

3.5. Combination therapy using AdRGD-IL12 and AdRGD-TNF α for B16BL6 melanoma

In our experimental model, the limiting dose of AdRGD-IL12 that demonstrated effective tumor regression without a rise in serum cytokine levels was 10^9 VP/tumor. We previously found that the limiting dose of AdRGD-TNF α was also 10^9 VP/tumor in a similar experiment [4]. Identification of a limiting dose is important for continued progress in research and development of the in vivo cytokine gene therapy. In order to further improve efficacy while remaining below the limiting dose, we must evaluate combination therapy using two or more vectors that express distinct cytokines and possess varying therapeutic mechanisms, rather than relying on the therapeutic effects of a single cytokine-expressing vector. Additionally, several reports demonstrated a concept to reinforce the anti-tumor efficacy in murine melanoma model by combination of IL-12 and TNF- α [36,37]. Therefore, we evaluated the effects of intratumoral co-injection of AdRGD-IL-12 and AdRGD-TNF α at the limiting dose or below. B16BL6 tumors injected with a mixture of 5×10^8 AdRGD-IL12 and 5×10^8 AdRGD-TNF α demonstrated more effective regression than tumors injected with either AdRGD-IL12 or AdRGD-TNF α alone at 10^9 VP (Fig. 6A). Furthermore, all six mice co-injected with 10^9 AdRGD-IL12 and 10^9 AdRGD-TNF α achieved complete regression of established B16BL6 tumors and remained tumor-free until day 90 after tumor challenge. On the other hand, no reduction

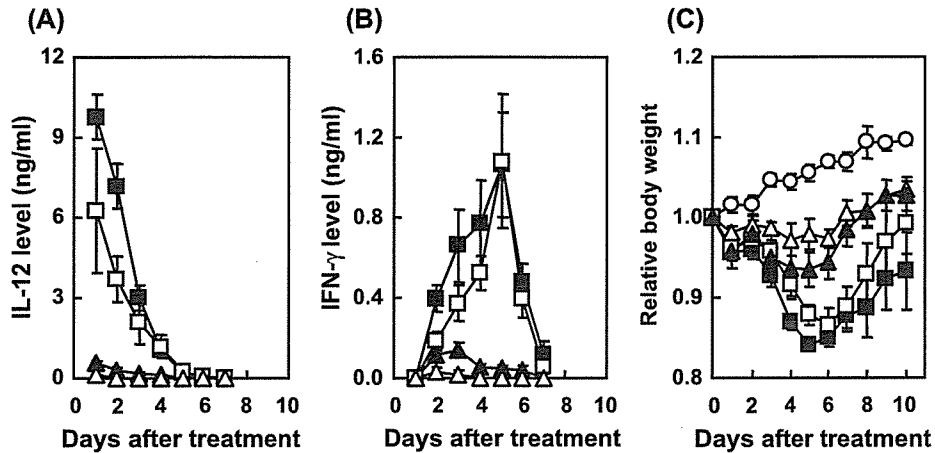


Fig. 5. IL-12 level (A) or IFN- γ level (B) in sera, and body weight change (C) upon intratumoral administration of Ad-IL12 or AdRGD-IL12 at 10^{10} or 10^{11} VP. B16BL6 cells were intradermally inoculated into C57BL/6 mice at 2×10^5 cells/mouse. The tumors (5–7 mm in diameter) were injected with Ad-IL12 [(Δ) 10^{10} , or (\square) 10^{11} VP/tumor], AdRGD-IL12 [(\blacktriangle) 10^{10} , or (\blacksquare) 10^{11} VP/tumor], or PBS (O). IL-12 (A) and IFN- γ (B) concentrations in sera from these mice were measured using the murine IL-12 ELISA kit and murine IFN- γ ELISA kit, respectively. Relative body weight (C) was calculated according to the formula described in Materials and methods. The data are representative of two independent experiments. Each point represents the mean \pm S.E. of five mice.

in body weight was observed in any group (Fig. 6B) and serum concentrations of IL-12 and TNF- α were less than the detection limit in mice co-injected with two vectors (data not shown). These results strongly suggest that intratumoral co-injection of multiple cytokine-expressing AdRGDs is a promising strategy capable of improving therapeutic efficacy and suppressing adverse effects of *in vivo* cytokine gene therapy for melanoma. In addition, other groups have also reported that the application of multiple cytokine genes could demonstrate synergistic therapeutic effects even if gene therapy using a single cytokine gene was ineffective [38–40].

In conclusion, in order to optimize *in vivo* cytokine gene therapy, we must examine the effectiveness and safety of single cytokine-expressing vectors and of multiple vector

combinations, which can be selected based on the mechanisms of efficacy and extent of adverse effects.

Acknowledgements

We are grateful to Dr. Hiroshi Yamamoto (Department of Immunology, Graduate School of Pharmaceutical Sciences, Osaka University) for providing mIL-12 BIA/pBluescript II KS(–), GK1.5 ascites, and 53-6.72 ascites; to Yasushige Masunaga (Department of Biopharmaceutics, Kyoto Pharmaceutical University) for technical assistance with the E-release assay; and to Kae Suzuki and Saki Tanaka (Department of Pharmaceutics, School of Pharmaceutical

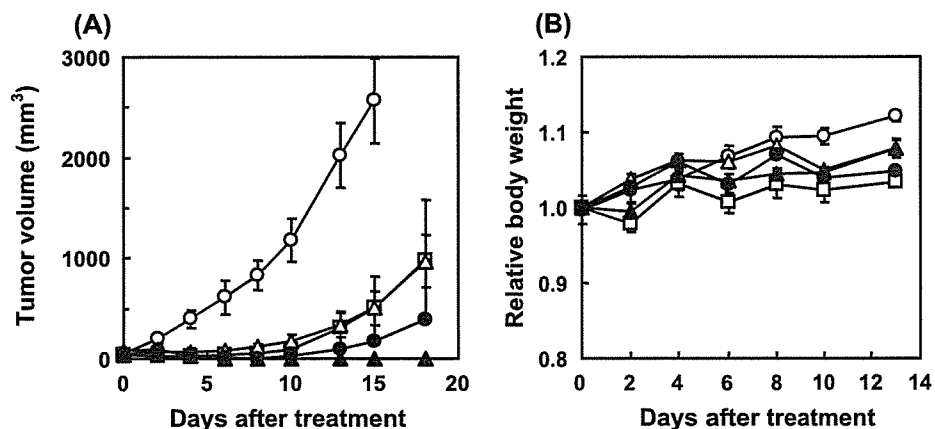


Fig. 6. Anti-B16BL6 tumor effect and body weight change in response to a combination of AdRGD-IL12 and AdRGD-TNF α . B16BL6 cells were intradermally inoculated into C57BL/6 mice at 2×10^5 cells/mouse. Six days later, the tumors were injected with 10^9 AdRGD-IL12 alone (Δ), 10^9 AdRGD-TNF α alone (\square), a combination of 5×10^8 AdRGD-IL12 and 5×10^8 AdRGD-TNF α (\bullet), a combination of 10^9 AdRGD-IL12 and 10^9 AdRGD-TNF α (\blacktriangle), or PBS (O). The tumor volume (A) and the relative body weight (B) were calculated according to the formula described in Materials and methods. The data are representative of two independent experiments. Each point represents the mean \pm S.E. of three to six mice.

Sciences, Mukogawa Women's University) for assistance with animal experiments.

This study was supported in part by grants from the Ministry of Health and Welfare in Japan.

References

- [1] A. Schneeberger, M. Goos, G. Stingl, S.N. Wagner, Management of malignant melanoma: new developments in immune and gene therapy, *Clin. Exp. Dermatol.* 25 (2000) 509–519.
- [2] J.K. Wildemore IV, L. Schuchter, R. Mick, M. Synnestvedt, R. Elenitsas, I. Bedrosian, B.J. Czerniecki, D. Guerry IV, S.R. Lessin, D.E. Elder, L.P. Bucky, Locally recurrent malignant melanoma characteristics and outcomes: a single-institution study, *Ann. Plast. Surg.* 46 (2001) 488–494.
- [3] Y. Okada, N. Okada, S. Nakagawa, H. Mizuguchi, K. Takahashi, N. Mizuno, T. Fujita, A. Yamamoto, T. Hayakawa, T. Mayumi, Tumor necrosis factor α -gene therapy for an established murine melanoma using RGD (Arg-Gly-Asp) fiber-mutant adenovirus vectors, *Jpn. J. Cancer Res.* 93 (2002) 436–444.
- [4] Y. Okada, N. Okada, H. Mizuguchi, T. Hayakawa, T. Mayumi, N. Mizuno, An investigation of adverse effects caused by the injection of high-dose TNF α -expressing adenovirus vector into established murine melanoma, *Gene Ther.* 10 (2003) 700–705.
- [5] U. Gubler, A.O. Chua, D.S. Schoenhaut, C.M. Dwyer, W. McComas, R. Motyka, N. Nabavi, A.G. Wolitzky, P.M. Quinn, P.C. Familletti, M.K. Gately, Coexpression of two distinct genes is required to generate secreted bioactive cytotoxic lymphocyte maturation factor, *Proc. Natl. Acad. Sci. U. S. A.* 88 (1991) 4143–4147.
- [6] S.F. Wolf, P.A. Temple, M. Kobayashi, D. Young, M. Dicig, L. Lowe, R. Dzialo, L. Fitz, C. Ferenz, R.M. Hewick, K. Kelleher, S.T. Herrmann, S.C. Clark, L. Azzoni, S.H. Chan, G. Trinchieri, B. Perussia, Cloning of cDNA for natural killer cell stimulatory factor, a heterodimeric cytokine with multiple biologic effects on T and natural killer cells, *J. Immunol.* 146 (1991) 3074–3081.
- [7] M.J. Robertson, R.J. Soiffer, S.F. Wolf, T.J. Manley, C. Donahue, D. Young, S.H. Herrmann, J. Ritz, Response of human natural killer (NK) cells to NK cell stimulatory factor (NKSF): cytolytic activity and proliferation of NK cells are differentially regulated by NKSF, *J. Exp. Med.* 175 (1992) 779–788.
- [8] M.J. Brunda, Interleukin-12, *J. Leukoc. Biol.* 55 (1994) 280–288.
- [9] S.H. Chan, B. Perussia, J.W. Gupta, M. Kobayashi, M. Pospisil, H.A. Young, S.F. Wolf, D. Young, S.C. Clark, G. Trinchieri, Induction of interferon- γ production by natural killer cell stimulatory factor: characterization of the responder cells and synergy with other inducers, *J. Exp. Med.* 173 (1991) 869–879.
- [10] S.H. Chan, M. Kobayashi, D. Santoli, B. Perussia, G. Rinchieri, Mechanisms of IFN- γ induction by natural killer cell stimulatory factor (NKSF/IL-12). Role of transcription and mRNA stability in the synergistic interaction between NKSF and IL-2, *J. Immunol.* 148 (1992) 92–98.
- [11] C.S. Hsieh, S.E. Macatonia, C.S. Tripp, S.F. Wolf, A. O'Garra, K.M. Murphy, Development of TH1 CD4⁺ T cells through IL-12 produced by Listeria-induced macrophages, *Science* 260 (1993) 547–549.
- [12] R.A. Seder, R. Gazzinelli, A. Sher, W.E. Paul, Interleukin 12 acts directly on CD4⁺ T cells to enhance priming for interferon γ production and diminishes interleukin 4 inhibition of such priming, *Proc. Natl. Acad. Sci. U. S. A.* 90 (1993) 10188–10192.
- [13] C.L. Nastala, H.D. Edington, T.G. McKinney, H. Tahara, M.A. Nalesnik, M.J. Brunda, M.K. Gately, S.F. Wolf, R.D. Schreiber, W.J. Storkus, Recombinant IL-12 administration induces tumor regression in association with IFN- γ production, *J. Immunol.* 153 (1994) 1697–1706.
- [14] E.E. Voest, B.M. Kenyon, M.S. O'Reilly, G. Truitt, R.J. D'Amato, J. Folkman, Inhibition of angiogenesis in vivo by interleukin 12, *J. Natl. Cancer Inst.* 87 (1995) 581–586.
- [15] J.P. Leonard, M.L. Sherman, G.L. Fisher, L.J. Buchanan, G. Larsen, M.B. Atkins, J.A. Sosman, J.P. Dutcher, N.J. Vogelzang, J.L. Ryan, Effects of single-dose interleukin-12 exposure on interleukin-12-associated toxicity and interferon- γ production, *Blood* 90 (1997) 2541–2548.
- [16] M.B. Atkins, M.J. Robertson, M. Gordon, M.T. Lotze, M. DeCoste, J.S. DuBois, J. Ritz, A.B. Sandler, H.D. Edington, P.D. Garzone, J.W. Mier, C.M. Canning, L. Battiato, H. Tahara, M.L. Sherman, Phase I evaluation of intravenous recombinant human interleukin 12 in patients with advanced malignancies, *Clin. Cancer Res.* 3 (1997) 409–417.
- [17] S. Obana, H. Miyazawa, E. Hara, T. Tamura, H. Nariuchi, M. Takata, S. Fujimoto, H. Yamamoto, Induction of anti-tumor immunity by mouse tumor cells transfected with mouse interleukin-12 gene, *Jpn. J. Med. Sci. Biol.* 48 (1995) 221–236.
- [18] H. Mizuguchi, M.A. Kay, Efficient construction of a recombinant adenovirus vector by an improved in vitro ligation method, *Hum. Gene Ther.* 9 (1998) 2577–2583.
- [19] H. Mizuguchi, M.A. Kay, A simple method for constructing E1- and E1/E4-deleted recombinant adenoviral vectors, *Hum. Gene Ther.* 10 (1999) 2013–2017.
- [20] H. Mizuguchi, N. Koizumi, T. Hosono, N. Utoguchi, Y. Watanabe, M.A. Kay, T. Hayakawa, A simplified system for constructing recombinant adenoviral vectors containing heterologous peptides in the HI loop of their fiber knob, *Gene Ther.* 8 (2001) 730–735.
- [21] J.V. Maizel Jr., D.O. White, M.D. Scharff, The polypeptides of adenovirus. I. Evidence for multiple protein components in the virion and a comparison of types 2, 7A, and 12, *Virology* 36 (1968) 115–125.
- [22] P. Janik, P. Briand, N.R. Hartmann, The effect of estrone-progesterone treatment on cell proliferation kinetics of hormone-dependent GR mouse mammary tumours, *Cancer Res.* 35 (1975) 3698–3704.
- [23] N. Okada, M. Tsujino, Y. Hagiwara, A. Tada, Y. Tamura, K. Mori, T. Saito, S. Nakagawa, T. Mayumi, T. Fujita, A. Yamamoto, Administration route-dependent vaccine efficiency of murine dendritic cells pulsed with antigens, *Br. J. Cancer* 84 (2001) 1564–1570.
- [24] D.P. Dialynas, Z.S. Quan, K.A. Wall, A. Pierres, J. Quintans, M.R. Loken, M. Pierres, F.W. Fitch, Characterization of the murine T cell surface molecule, designated L3T4, identified by monoclonal antibody GK1.5: similarity of L3T4 to the human Leu-3/T4 molecule, *J. Immunol.* 131 (1983) 2445–2451.
- [25] J.A. Ledbetter, L.A. Herzenberg, Xenogeneic monoclonal antibodies to mouse lymphoid differentiation antigens, *Immunol. Rev.* 47 (1979) 63–90.
- [26] M.A. Kay, S.L. Woo, Gene therapy for metabolic disorders, *Trends Genet.* 10 (1994) 253–257.
- [27] K.F. Kozarsky, J.M. Wilson, Gene therapy: adenovirus vectors, *Curr. Opin. Genet. Dev.* 3 (1993) 499–503.
- [28] B. Breyer, W. Jiang, H. Cheng, L. Zhou, R. Paul, T. Feng, T.C. He, Adenoviral vector-mediated gene transfer for human gene therapy, *Curr. Gene Ther.* 1 (2001) 149–162.
- [29] S.A. Vorburger, K.K. Hunt, Adenoviral gene therapy, *Oncologist* 7 (2002) 46–59.
- [30] K. Benihoud, P. Yeh, M. Perricaudet, Adenovirus vectors for gene delivery, *Curr. Opin. Biotechnol.* 10 (1999) 440–447.
- [31] Y. Okada, N. Okada, S. Nakagawa, H. Mizuguchi, M. Kanehira, N. Nishino, K. Takahashi, N. Mizuno, T. Hayakawa, T. Mayumi, Fiber-mutant technique can augment gene transduction efficacy and anti-tumor effects against established murine melanoma by cytokine-gene therapy using adenovirus vectors, *Cancer Lett.* 177 (2002) 57–63.
- [32] N. Chattopadhyay, A. Chatterjee, Studies on the expression of $\alpha v \beta 3$ integrin receptors in non-malignant and malignant human cervical tumor tissues, *J. Exp. Clin. Cancer Res.* 20 (2001) 269–275.
- [33] M.D. Sachs, K.A. Rauen, M. Ramamurthy, J.L. Dodson, A.M. De Marzo, M.J. Putzi, M.P. Schoenberg, R. Rodriguez, Integrin αv

- and coxsackie adenovirus receptor expression in clinical bladder cancer, *Urology* 60 (2002) 531–536.
- [34] K.A. Rauen, D. Sudilovsky, J.L. Le, K.L. Chew, B. Hann, V. Schmitt, L.D. Schmitt, F. McCormick, Expression of the coxsackie adenovirus receptor in normal prostate and in primary and metastatic prostate carcinoma: potential relevance to gene therapy, *Cancer Res.* 62 (2002) 3812–3818.
- [35] Y.S. Haviv, J.L. Blackwell, A. Kanerva, P. Nagi, V. Krasnykh, I. Dmitriev, M. Wang, S. Naito, X. Lei, A. Hemminki, D. Carey, D.T. Curiel, Adenoviral gene therapy for renal cancer requires retargeting to alternative cellular receptors, *Cancer Res.* 62 (2002) 4273–4281.
- [36] W. Lasek, W. Feleszko, J. Gołab, T. Stokłosa, M. Marczak, A. Dąbrowska, M. Malejczyk, M. Jakóbiśiak, Antitumor effects of the combination immunotherapy with interleukin-12 and tumor necrosis factor α in mice, *Cancer Immunol. Immunother.* 45 (1997) 100–108.
- [37] W. Lasek, A. Mackiewicz, A. Czajka, T. Świtaj, J. Gołab, M. Wiznerowicz, G. Korczak-Kowalska, E.Z. Bakowicz-Iskra, K. Gryśka, D. Iżycki, M. Jakóbiśiak, Antitumor effects of the combination therapy with TNF- α gene-modified tumor cells and interleukin 12 in a melanoma model in mice, *Cancer Gene Ther.* 7 (2000) 1581–1590.
- [38] C.L. Addison, J.L. Bramson, M.M. Hitt, W.J. Muller, J. Gaudie, F.L. Graham, Intratumoral coinjection of adenoviral vectors expressing IL-2 and IL-12 results in enhanced frequency of regression of injected and untreated distal tumors, *Gene Ther.* 5 (1998) 1400–1409.
- [39] P.C. Emtage, Y. Wan, M. Hitt, F.L. Graham, W.J. Muller, A. Zlotnik, J. Gaudie, Adenoviral vectors expressing lymphotactin and interleukin 2 or lymphotactin and interleukin 12 synergize to facilitate tumor regression in murine breast cancer models, *Hum. Gene Ther.* 10 (1999) 697–709.
- [40] Y. Liu, H. Huang, A. Saxena, J. Xiang, Intratumoral coinjection of two adenoviral vectors expressing functional interleukin-18 and inducible protein-10, respectively, synergizes to facilitate regression of established tumors, *Cancer Gene Ther.* 9 (2002) 533–542.



Anti-tumor activity of chemokine is affected by both kinds of tumors and the activation state of the host's immune system: implications for chemokine-based cancer immunotherapy[☆]

Naoki Okada,^{a,*} Jian-Qing Gao,^{b,c,*} Akinori Sasaki,^a Masakazu Niwa,^a Yuka Okada,^d Takashi Nakayama,^c Osamu Yoshie,^e Hiroyuki Mizuguchi,^f Takao Hayakawa,^g Takuya Fujita,^a Akira Yamamoto,^a Yasuo Tsutsumi,^b Tadanori Mayumi,^b and Shinsaku Nakagawa^{b,*}

^a Department of Biopharmaceutics, Kyoto Pharmaceutical University, 5 Nakauchi-cho, Misasagi, Yamashina-ku, Kyoto 607-8414, Japan

^b Department of Biopharmaceutics, Graduate School of Pharmaceutical Sciences, Osaka University, 1-6 Yamadaoka, Suita, Osaka 565-0871, Japan

^c Department of Pharmaceutics, School of Pharmaceutical Sciences, Zhejiang University, 353 Yanan Road, Hangzhou, Zhejiang 310031, PR China

^d Department of Pharmaceutics, School of Pharmaceutical Sciences, Mukogawa Women's University,

11-68 Kyuban-cho, Koshien, Nishinomiya, Hyogo 663-8179, Japan

^e Department of Microbiology, Kinki University School of Medicine, Osaka-Sayama, Osaka 589-8511, Japan

^f Division of Cellular and Gene Therapy Products, National Institute of Health Sciences, 1-18-1 Kamiyoga, Setagaya-ku, Tokyo 158-8501, Japan

^g National Institute of Health Sciences, 1-18-1 Kamiyoga, Setagaya-ku, Tokyo 158-8501, Japan

Received 23 February 2004

Abstract

In this study, we screened the anti-tumor activity of murine chemokines including CCL17, CCL19, CCL20, CCL21, CCL22, CCL27, XCL1, and CX3CL1 by inoculating murine B16BL6, CT26, or OV-HM tumor cells, all of which were transfected with chemokine-expressing fiber-mutant adenovirus vector, into immunocompetent mice. A tumor-suppressive effect was observed in mice inoculated with CCL19/B16BL6 and XCL1/B16BL6, and CCL22/OV-HM showed considerable retardation in tumor growth. In the cured mice inoculated with CCL22/OV-HM, a long-term specific immune protection against parental tumor was developed. However, we were unable to identify the chemokine that had a suppressive activity common to all three tumor models. Furthermore, an experiment using chemokine-transfected B16BL6 cells was also performed on mice sensitized with melanoma-associated antigen. A drastic enhancement of the frequency of complete rejection was observed in mice inoculated with CCL17-, CCL19-, CCL22-, and CCL27-transfected B16BL6. Altogether, our results suggest that the tumor-suppressive activity of chemokine-gene immunotherapy is greatly influenced by the kind of tumor and the activation state of the host's immune system.

© 2004 Elsevier Inc. All rights reserved.

Keywords: Adenovirus vector; Chemokine; Transfection; Anti-tumor activity; Gene immunotherapy

[☆] **Abbreviations:** Ad, adenovirus vector; AdRGD, RGD fiber-mutant Ad; CTL, cytotoxic T lymphocyte; DC, dendritic cell; FBS, fetal bovine serum; MOI, multiplicity of infection; NK, natural killer; PBS, phosphate-buffered saline; TCID₅₀, tissue culture infectious dose₅₀.

* Corresponding authors. Fax: +81-75-595-4761 (N. Okada), +81-6-6879-8179 (S. Nakagawa), +86-571-87217376 (J.-Q. Gao).

E-mail addresses: okada@mb.kyoto-phu.ac.jp (N. Okada), gaojq@phs.osaka-u.ac.jp (J.-Q. Gao), nakagawa@phs.osaka-u.ac.jp (S. Nakagawa).

Chemokine consists of a superfamily of small (8–14 kDa), secreted basic proteins that regulate relevant leukocyte-migration and -invasion into tissue by interacting with their specific receptors, which belong to the superfamily of seven-transmembrane domain G-protein-coupled receptors [1,2]. The function of chemokine, which is capable of attracting specific immune cells, is demonstrated in inflammatory disease sites as well as normal lymphoid tissues [2]. Because of these properties, chemokine is considered as the intriguing molecule for cancer immunotherapy, which is based on the premise of

the eradication of tumor cells as a consequence of interaction with immune cells that have migrated and accumulated in tumor tissues [3]. To date, more than 40 chemokines have been identified, and several chemokines have been demonstrated as candidates for cancer treatment for use either as sole agents or with an adjuvant [4–8].

We hypothesized that efficient *in vitro* transfection of chemokine gene into tumor cells could render the tumor sufficient chemokine expression *in vivo* for screening anti-tumor activity. The chemokine, secreted from inoculated tumor cells, would induce the accumulation of immune cells in the tumor tissue. Consequently, the interaction between the immune cells and the tumor cells should initiate and/or demonstrate the anti-tumor immune response. Among the various methods of gene transduction, recombinant adenovirus vector (Ad) can provide high-level transduction efficacy to a variety of cell types [9,10]. However, some tumor cells exhibit a resistance to Ad-mediated gene transduction due to a decline in the expression of a coxsackie-adenovirus receptor, a primary Ad-receptor, on their surface. We previously demonstrated that, compared with conventional Ad, the fiber-mutant Ad harboring the RGD sequence in the HI loop of the fiber knob (AdRGD) could more efficiently transduce foreign genes into several kinds of tumor cells due to their directivity to α v-integrin positive in the majority of tumors [11–13]. Therefore, chemokine-expressing AdRGD would be useful not only for screening the anti-tumor activity of chemokines by *in vitro* transfection, but also for developing *in vivo* cancer gene immunotherapy.

In the present study, we first confirmed the vector performance of eight AdRGDs encoding each mouse chemokine, CCL17, CCL19, CCL20, CCL21, CCL22, CCL27, XCL1, or CX3CL1. The anti-tumor activity of these chemokines was investigated in mice by inoculating three kinds of murine tumor cells, B16BL6 melanoma, CT26 colon carcinoma, and OV-HM ovarian carcinoma cells, transfected with each chemokine-expressing AdRGD. In addition, we examined the growth and rejection ratio of chemokine gene-transduced B16BL6 cells in mice sensitized with melanoma-associated antigen (gp100).

Materials and methods

Cell lines and animals. Human lung carcinoma A549 cells were purchased from ATCC (Manassas, VA, USA). Murine melanoma B16BL6 cells (H-2^b) and human embryonic kidney 293 cells were obtained from JCRB cell bank (Tokyo, Japan). Murine colon carcinoma CT26 cells (H-2^d) were kindly provided by Dr. Nicholas P. Restifo (National Cancer Institute, Bethesda, MD, USA). Murine ovarian carcinoma OV-HM cells (H-2^{b/k}) were kindly provided by Dr. Hiromi Fujiwara (School of Medicine, Osaka University, Osaka, Japan). A549 and 293 cells were maintained in Dulbecco's modified Eagle's medium supplemented with 10% fetal bovine serum (FBS) and antibiotics.

B16BL6 cells were cultured in a minimum essential medium supplemented with 7.5% FBS and antibiotics. CT26 and OV-HM cells were grown in an RPMI 1640 medium supplemented with 10% FBS and antibiotics. Murine pre-B lymphoma L1.2 cells and their stable transfectants of a specific chemokine receptor, L1.2/CCR4, L1.2/CCR6, L1.2/CCR7, L1.2/CCR10, L1.2/XCR1, and L1.2/CX3CR1 cells [14], were maintained in an RPMI 1640 medium supplemented with 10% FBS, 50 μ M of 2-mercaptoethanol, and antibiotics. All the cell lines were cultured at 37°C in a humidified atmosphere with 5% CO₂. Female C57BL/6 (H-2^b), BALB/c (H-2^d), and B6C3F1 (H-2^{b/k}) mice, ages 7–8 weeks, were purchased from SLC (Hamamatsu, Japan). All of the animal experimental procedures were in accordance with the Osaka University guidelines for the welfare of animals in experimental neoplasia.

Vectors. Replication-deficient AdRGD was based on the adenovirus serotype 5 backbone with deletions of E1/E3 region. The RGD sequence for α v-integrin-targeting was inserted into the HI loop of the fiber knob using a two-step method as previously described [11]. Mouse cDNAs of CCL17, CCL19, CCL20, CCL21, CCL22, and XCL1 were obtained from pExCell-mCCL17, pT7T3D-Pac-mCCL19, pFastBac1-mCCL20, pT7T3D-Pac-mCCL21, pBluescript SK(+)-mCCL22, and pExCell-mXCL1, respectively. The expression cassette containing each mouse chemokine cDNA under the control of the cytomegalovirus promoter was inserted into E1-deletion site for constructing AdRGD-CCL17, -CCL19, -CCL20, -CCL21, -CCL22, and -XCL1, respectively, by an improved *in vitro* ligation method as previously described [15,16]. Mouse CCL27-expressing AdRGD (AdRGD-CCL27), mouse CX3CL1-expressing AdRGD (AdRGD-CX3CL1), gp100-expressing AdRGD (AdRGD-gp100), β -galactosidase-expressing AdRGD (AdRGD-LacZ), luciferase-expressing AdRGD (AdRGD-Luc), and AdRGD-Null, which is identical to the AdRGD vectors without the gene expression cassette, were previously constructed [11,17–19]. AdRGD-LacZ, -Luc, and -Null were used as negative control vectors in the present study. All recombinant AdRGDs were propagated in 293 cells, purified by two rounds of cesium chloride gradient ultracentrifugation, dialyzed, and stored at –80°C. Titers (tissue culture infectious dose₅₀; TCID₅₀) of infective AdRGD particles were evaluated by the end-point dilution method using 293 cells.

RT-PCR analysis. A549 cells were transfected with each AdRGD at an MOI (multiplicity of infection; TCID₅₀/cell) of 50 for 2 h, and then the cells were washed twice with phosphate-buffered saline (PBS) and cultured for 24 h. The expression of mouse chemokine mRNA in these A549 cells was confirmed by an RT-PCR analysis as follows: total RNA was isolated from transduced A549 cells using Sepasol-RNA I Super (Nacalai Tesque, Kyoto, Japan) according to the manufacturer's instructions, following which RT proceeded for 60 min at 42°C in a 50- μ l reaction mixture containing 5 μ g total RNA treated with DNase I, 10 μ l of 5 \times RT buffer, 5 mM MgCl₂, 1 mM dNTP mix, 1 μ M random hexamers, 1 μ M oligo(dT), and 100 U ReverTra Ace (Toyobo, Osaka, Japan). PCR amplification of each mouse chemokine and human β -actin transcripts was performed in 50 μ l of a reaction mixture containing 1 μ l of RT-material, 5 μ l of 10 \times PCR buffer, 1.25 U Taq DNA polymerase (Toyobo), 1.5 mM MgCl₂, 0.2 mM dNTP, and 0.4 μ M primers. The sequences of the specific primers used for PCR amplification and the expected PCR product sizes are defined in Table 1. After denaturation for 2 min at 95°C, 30 (mouse chemokine) or 20 (human β -actin) cycles of denaturation for 30 s at 95°C, annealing for 30 s at 55°C (human β -actin), 60°C (mouse CCL17, CCL19, CCL20, CCL22, and CX3CL1), 62°C (mouse CCL21 and XCL1), or 63°C (mouse CCL27), and extension for 30 s at 72°C were repeated and followed by completion for 4 min at 72°C. The PCR product was electrophoresed on a 3% agarose gel, stained with ethidium bromide, and visualized under ultraviolet radiation. EZ Load (Bio-Rad, Tokyo, Japan) was used as a 100 bp molecular ruler.

***In vitro* chemotaxis assay.** A549 cells were transfected with each AdRGD at an MOI of 50 for 2 h, and then the cells were washed twice with PBS and cultured in media containing 10% FBS. After 24 h

Table 1
Primer sequences used for PCR amplification

Gene	Primer sequence (5' → 3')	Product size (bp)
Mouse CCL17	(F) TGC TTC TGG GGA CTT TTC TG (R) CCT TGG GTT TTT CAC CAA TC	242
Mouse CCL19	(F) GAA AGC CTT CCG CTA CCT TC (R) TGC TGT TGC CTT TGT TCT TG	164
Mouse CCL20	(F) CGA CTG TTG CCT CTC GTA CA (R) CAC CCA GTT CTG CTT TGG AT	157
Mouse CCL21	(F) CTG AGC CTC CTT AGC CTG GT (R) TCC TCT TGA GGG CTG TGT CT	381
Mouse CCL22	(F) TAT GGT GCC AAT GTG GAA GA (R) GCA GGA TTT TGA GGT CCA GA	102
Mouse CCL27	(F) CTC CCG CTG TTA CTG TTG CT (R) AGT TTT GCT GTT GGG GGT TT	331
Mouse XCL1	(F) ATG GGT TGT GGA AGG TGT G (R) GGG AAC AGT TTC AGC CAT GT	250
Mouse CX3CL1	(F) GCA GTG ACC GGA TCA TCT CT (R) GGC ACC AGG ACG TAT GAG TT	701
Human β -actin	(F) CCT TCC TGG GCA TGG AGT CCT G (R) GGA GCA ATG ATC TTG ATC TTC	202

cultivation, cells were washed and incubated with an assay medium (phenol red-free RPMI 1640 containing 0.5% bovine serum albumin and 20 mM Hepes, pH 7.4) for another 24 h. The resulting conditioned medium was collected, and its chemoattractant activity was measured by an in vitro chemotaxis assay across a polycarbonate membrane with 5- μ m pores (Chemotaxicell-24; Kurabo, Osaka, Japan) using L1.2 transfectants expressing the specific receptor for chemokines. Recombinant chemokines corresponding to each specific receptor (mouse: CCL19, CCL20, CCL22, CCL27, XCL1, and CX3CL1) were purchased from DakoCytomation (Kyoto, Japan) and used as a positive control for cell migration. Migration was allowed for 2 h at 37 °C in a 5% CO₂ atmosphere. The migrated cells were lysed and quantitated using a PicoGreen dsDNA quantitation reagent (Invitrogen, Tokyo, Japan), and the migration activity was expressed in term of the percentage of the input cells calculated by the following formula: (% of input cells) = (the number of migrated cells)/(the number of cells placed in Chemotaxicell-24; 1×10^6 cells) \times 100.

Evaluation of growth of chemokine gene-transduced tumor cells in immunocompetent mice. B16BL6, CT26, and OV-HM cells were transfected with each AdRGD at an MOI of 400, 50, and 10, respectively. After 24 h cultivation, the cells were harvested and washed three times with PBS, and then 2×10^5 transduced B16BL6 cells, 2×10^5 transduced CT26 cells, and 1×10^6 transduced OV-HM cells were intradermally inoculated into the flank of C57BL/6 mice, BALB/c mice, and B6C3F1 mice, respectively. The major and minor axes of the tumor were measured using microcalipers, and the tumor volume was calculated by the following formula: (tumor volume; mm³) = (major axis; mm) \times (minor axis; mm)² \times 0.5236 [20]. The mice were euthanized when one of the two measurements was greater than 15 mm. On day 60 after tumor inoculation, the tumor-free mice were judged as individuals that could achieve complete rejection. In some cases, the mice that could completely reject a primary tumor were rechallenged by intradermal injection into the flank with 1×10^6 parental or irrelevant tumor cells without chemokine gene-transduction at 3 months after the initial challenge.

Evaluation of growth and rejection ratio of chemokine gene-transduced B16BL6 cells in mice sensitized with melanoma-associated antigen. The immunization of mice with melanoma-associated antigen was performed by the administration of dendritic cells (DCs) transduced

with the gp100 gene. The isolation, cultivation, and gene transduction procedures for C57BL/6 mouse bone marrow-derived DCs conformed to the methods previously described [21]. DCs transfected with AdRGD-gp100 at an MOI of 50 for 2 h were intradermally injected into the right flank of C57BL/6 mice at 5×10^5 cells/50 μ l. At 1 week after the vaccination, 2×10^5 intact or transduced B16BL6 cells were inoculated into the left flank of the mice. The tumor growth and complete rejection were assessed as described above.

Results

Expression of chemokine mRNA and protein in cells transfected with AdRGD

In order to verify the vector performance of mouse chemokine gene-carried AdRGDs, we first examined

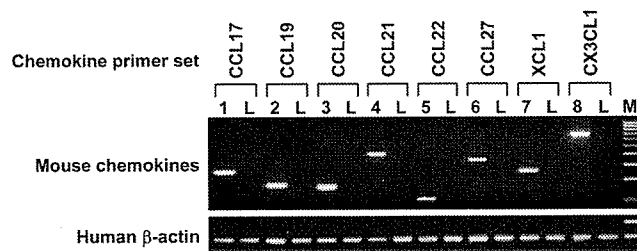


Fig. 1. RT-PCR analysis of chemokine mRNA expression in A549 cells transfected with each chemokine gene-carried AdRGD. PCR for mouse chemokine and human β -actin transcripts was performed on the same RT samples using each specific primer set (summarized in Table 1) to ensure the quality of the procedure. Lane L is negative control using AdRGD-LacZ-transfected A549 (LacZ/A549) cell-derived RT material. Lanes 1–8 represent CCL17/A549, CCL19/A549, CCL20/A549, CCL21/A549, CCL22/A549, CCL27/A549, XCL1/A549, and CX3CL1/A549, respectively. Lane M is a 100 bp molecular ruler.

mRNA expression in transfected cells by an RT-PCR analysis (Fig. 1). In this experiment, human lung carcinoma A549 cells were used instead of murine tumor cells to eliminate the influence of the expression of endogenous mouse chemokine. A549 cells transfected with AdRGD-CCL17, -CCL19, -CCL20, -CCL21, -CCL22, -CCL27, -XCL1, or -CX3CL1 expressed corresponding mouse chemokine mRNA, whereas no PCR products derived from the transcripts of the mouse chemokine gene were detected in AdRGD-LacZ-transfected A549 cells. Next, using in vitro chemotaxis assay, we investi-

gated whether A549 cells transfected with each chemokine gene-carried AdRGD could secrete chemokine protein as a biologically active form into culture supernatants. As shown in Fig. 2, the culture supernatants of each chemokine gene-transduced A549 cell could induce greater migration of cells expressing the corresponding chemokine receptor than those of the intact A549 cells or the AdRGD-Luc-transfected A549 (Luc/A549) cells. The migration of parental L1.2 cells for chemokine receptor-transfectants was not observed in recombinant chemokine-added wells, and they were

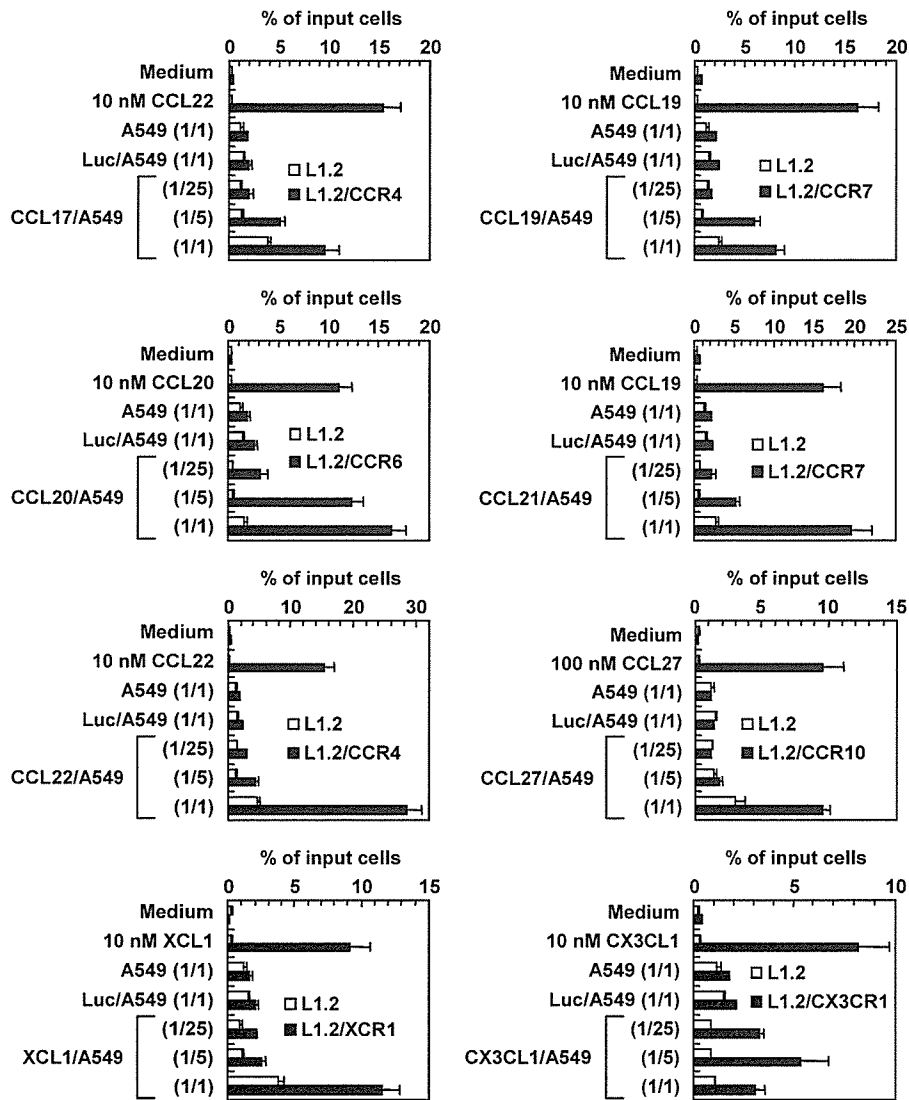


Fig. 2. Chemoattractant activity of culture supernatants of A549 cells transfected with each chemokine gene-carried AdRGD against the stable specific chemokine receptor-expressing cells. The culture supernatants of intact A549 cells, AdRGD-Luc-transfected A549 (Luc/A549) cells, and chemokine gene-transduced A549 cells were prepared and diluted with an assay medium. The fractional values with parentheses in each panel express the dilution factor. These samples and recombinant chemokines dissolved with the assay medium were added to a 24-well culture plate. Cells expressing specific receptors for CCL17 and CCL22 (L1.2/CCR4), CCL20 (L1.2/CCR6), CCL19 and CCL21 (L1.2/CCR7), CCL27 (L1.2/CCR10), XCL1 (L1.2/XCR1), or CX3CL1 (L1.2/CX3CR1) were suspended with the assay medium and placed in a Chemotaxicell-24 installed on each well at 1×10^6 cells. Likewise, parental L1.2 cells for these transfectants were prepared and added to Chemotaxicell-24. Cell migration was allowed for 2 h at 37 °C in a 5% CO₂ atmosphere. The cells that migrated to the lower well were lysed and quantitated using a PicoGreen dsDNA quantitation reagent. The data are expressed as means \pm SE of the triplicate results.

maintained at low levels against the culture supernatants of intact A549, Luc/A549, and chemokine gene-transduced A549 cells. These results clearly demonstrated that all AdRGDs encoding each chemokine gene could deliver the concerned gene to target cells, and that transfected cells could secrete the chemokine protein which maintained original chemoattractant activity.

In vivo anti-tumor effect by transfection with chemokine-expressing AdRGD

B16BL6 and CT26 cells were each transfected with eight kinds of chemokine-expressing AdRGDs and AdRGD-Luc, as a control vector, at an MOI of 400 and 50, respectively. OV-HM cells were transfected with

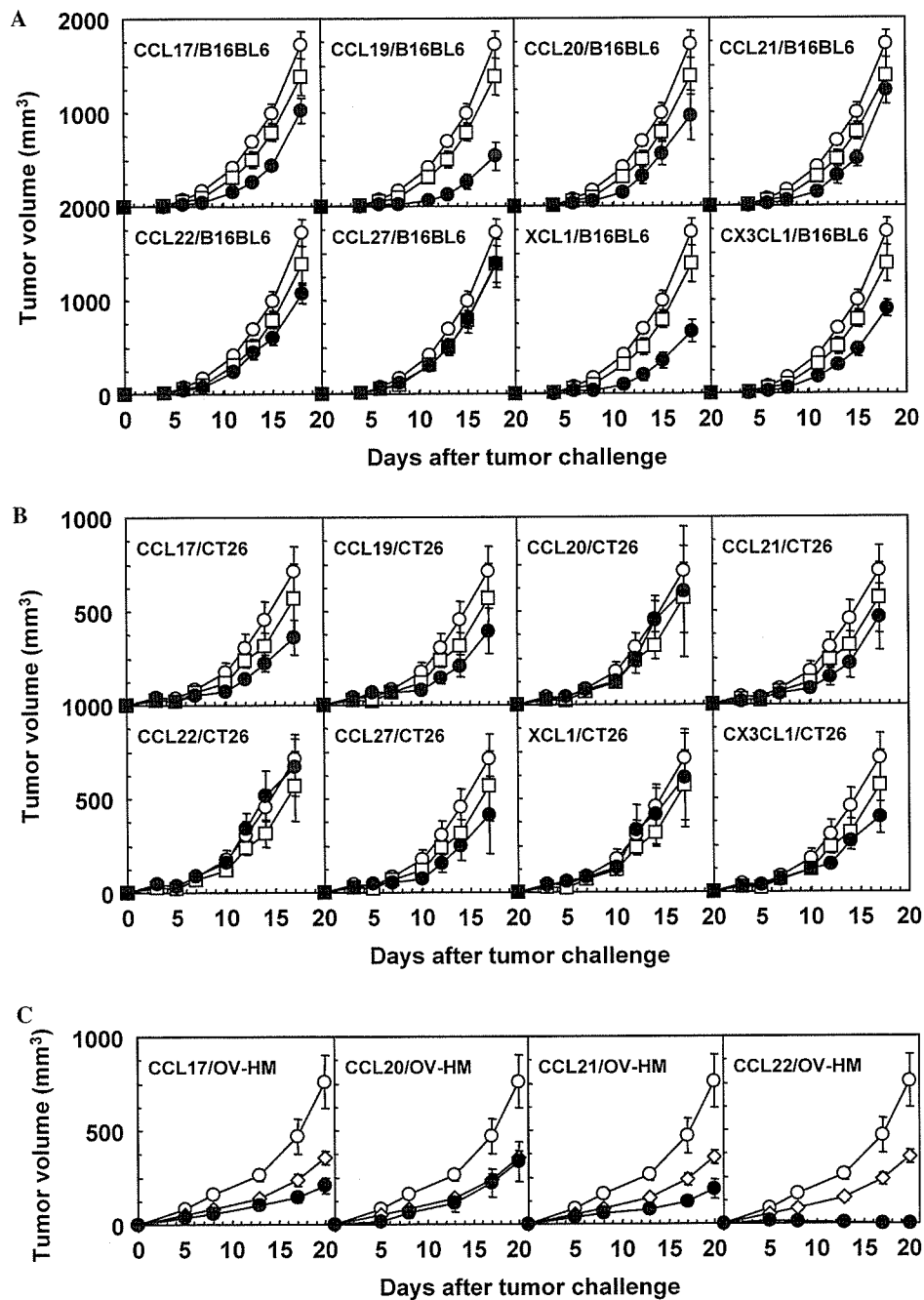


Fig. 3. In vivo growth of three kinds of murine tumor cells transduced with the chemokine gene. B16BL6 cells (A), CT26 cells (B), and OV-HM cells (C) were transfected with each chemokine-expressing AdRGD at an MOI of 400, 50, and 10, respectively, for 24 h. C57BL/6 mice, BALB/c mice, and B6C3F1 mice were intradermally injected in the flank with 2×10^5 transduced B16BL6 cells, 2×10^5 transduced CT26 cells, and 1×10^6 transduced OV-HM cells (●), respectively. Similarly, mice were inoculated with three kinds of intact tumor cells (○), AdRGD-Luc-transfected B16BL6 cells or CT26 cells (□), or AdRGD-Null-transfected OV-HM cells (◇), as control groups. The tumor volume was calculated after measuring the major and minor axes of the tumor at indicated points. Each point represents the mean \pm SE of 6–10 mice. The data are representative of two independent experiments.

AdRGD-CCL17, -CCL20, -CCL21, -CCL22, or control AdRGD-Null at an MOI of 10. These transduced tumor cells were intradermally inoculated into H-2 haplotype-matched mice, and tumor growth was compared with that of intact tumors. As shown in Fig. 3, the tumorigenicity of B16BL6 and CT26 cells was hardly affected by transfection with the control vector, whereas OV-HM cells transfected with AdRGD-Null exhibited a slight delay of tumor growth as compared with intact OV-HM cells. Among 20 combinations of chemokine and tumor cells, an obvious tumor-suppressive effect was recognized in mice inoculated with CCL19/B16BL6, XCL1/B16BL6, or CCL22/OV-HM cells. In contrast, the *in vivo* growth of CCL27/B16BL6, CCL20/CT26, CCL22/CT26, XCL1/CT26, and CCL20/OV-HM cells was the same as that of the control vector-transfected cells, and only a slight delay of tumor growth was

observed in five B16BL6 groups (CCL17, CCL20, CCL21, CCL22, and CX3CL1), five CT26 groups (CCL17, CCL19, CCL21, CCL27, and CX3CL1), and two OV-HM groups (CCL17 and CCL21). Importantly, CCL22/OV-HM cells not only demonstrated considerable retardation in tumor growth but were also completely rejected in 9 of 10 mice. In the rechallenge experiment, these cured mice were intradermally injected with 1×10^6 parental OV-HM cells or irrelevant B16BL6 cells at 3 months after the initial challenge. Five of six mice rechallenged with OV-HM cells remained tumor-free for more than 2 months, whereas rechallenging with B16BL6 cells perfectly developed palpable tumors in three additional mice within 2 weeks (data not shown). These results indicate the generation of long-term specific immunity against OV-HM tumor in mice that could once reject CCL22/OV-HM cells.

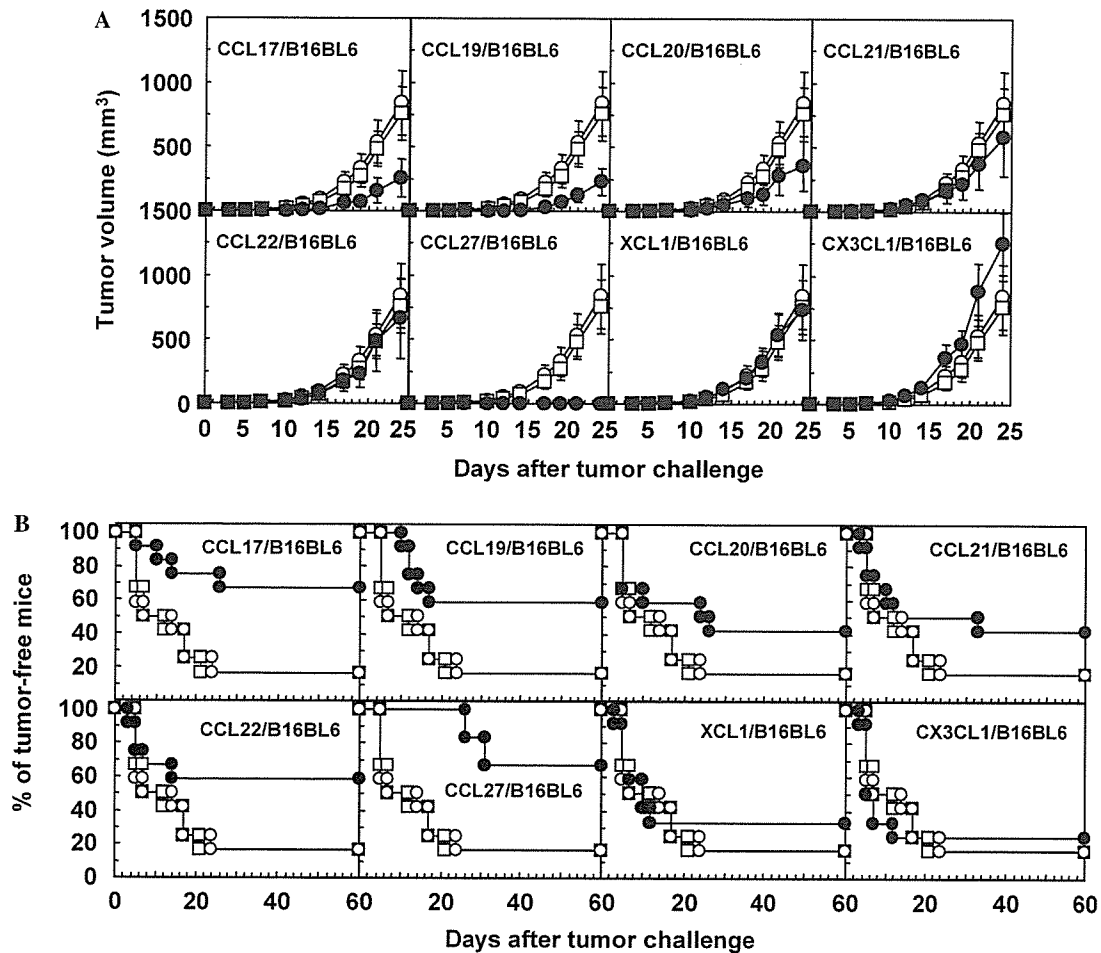


Fig. 4. Growth and rejection ratio of B16BL6 cells transduced with the chemokine gene in mice primed with melanoma-associated antigen. C57BL/6 mouse bone marrow-derived DCs were transfected with AdRGD-gp100 at an MOI of 50 for 2 h and they were intradermally injected into the right flank of syngeneic mice at 5×10^5 cells. At 1 week after the vaccination, these mice were intradermally inoculated in the left flank with 2×10^5 B16BL6 cells transfected with each chemokine-expressing AdRGD at an MOI of 400 for 24 h (●). Likewise, intact B16BL6 cells (○) or AdRGD-Luc-transfected B16BL6 cells (□) were inoculated in the gp100-primed mice, which were used as control groups. (A) The tumor volume was assessed three times per week. Each point represents the mean \pm SE of results obtained from 12 mice. (B) Data are expressed in terms of the percentage of mice without visible tumor against the total mice tested in each group.

Growth and rejection ratio of chemokine gene-transfected B16BL6 cells in gp100-primed mice

For the purpose of examining the influence of chemokine against tumor growth in hosts specifically sensitized with tumor-associated antigen, B16BL6 cells transfected with chemokine-expressing AdRGD were inoculated into mice that were vaccinated with DCs presenting gp100, one of the identified melanoma-associated antigens. As shown in Fig. 4A, CCL17-, CCL19-, or CCL27-transfection was very effective for tumor growth suppression in gp100-primed mice, whereas AdRGD-Luc-transfected B16BL6 cells did not show any difference in tumor growth as compared with intact cells. A remarkable enhancement was observed in the complete rejection ratio at 2 months after tumor inoculation in the CCL22-transfected group as well as in the CCL17, CCL19, and CCL27 groups (Fig. 4B). Also, transfection with AdRGD-CCL20 or -CCL21 moderately improved the rejection ratio of B16BL6 cells in gp100-primed mice. XCL1 did not show a notable difference in both the growth and the rejection ratio of B16BL6 cells as compared with the control groups, and CX3CL1-transfected cells showed a tendency to promote tumor growth as compared with the intact B16BL6 cells.

Discussion

The application of chemokines to cancer immunotherapy has recently attracted great attention, because of their chemoattractant activity for a variety of immune cells as well as the angiostatic activity of some chemokines such as CXCL9 and CXCL10. In addition, it has been known that some tumor cells express a lower level of chemokines than normal cells [22]. Therefore, we may obtain novel cancer gene immunotherapy capable of demonstrating an excellent therapeutic effect, if a specific chemokine is adequately expressed at a local tumor site by gene transduction. The tumor-suppressive activity of several chemokines was observed in actuality in various experimental tumor models using the *in vitro* transfection method [8,23–27]. We also previously demonstrated that a CC family chemokine, CCL27, could suppress OV-HM tumor growth via transfection into the tumor cells due to the local recruitment of T cells and natural killer (NK) cell, whereas the transfection of CX3CL1 did not show a significant effect [19]. However, there are few reports comparing the antitumor activity of a specific chemokine between distinct tumor models.

Thus, we screened the potential anti-tumor activity of CCL17, CCL19, CCL20, CCL21, CCL22, CCL27, XCL1, and CX3CL1 in three murine tumor models by *in vitro* transfection. In order to efficiently transduce the

chemokine gene into tumor cells, we constructed the AdRGDs carrying an expression cassette containing each murine chemokine cDNA by an improved *in vitro* ligation method. AdRGD can enhance gene transduction efficiency against a variety of tumor cells as compared with conventional Ad because of the expression of the RGD sequence, the α v-integrin-targeting peptide, at the HI-loop in their fiber knob [11–13]. Moreover, the improved *in vitro* ligation method enables speedy construction of a series of AdRGDs for screening by easy insertion of the expression cassette for the concerned gene into E1-deletion site [15,16]. With respect to the RT-PCR analysis and *in vitro* chemotaxis assay, transfection using our eight AdRGDs encoding the chemokine gene allowed tumor cells to express each corresponding chemokine mRNA and secrete a specific chemokine protein in a biologically active form (Figs. 1 and 2). Murine B16BL6 melanoma, murine CT26 colon carcinoma, and murine OV-HM ovarian carcinoma cells were transfected with chemokine-expressing AdRGDs at the MOI, which was suitable for adequately introducing a reporter gene into each tumor cell in preliminary examinations. To address the possibility of growth suppression depending on the cytotoxicity by AdRGD itself or secreted chemokine, we evaluated the viability of tumor cells transfected with each AdRGD at 48 h after transfection by MTT assay. The *in vitro* growth of the transfected cells was essentially identical to that of the intact cells with the exception of the OV-HM cells transduced with AdRGD-CCL19 or -XCL1 (data not shown). Therefore, CCL19 and XCL1 were excluded from the *in vivo* experiment using OV-HM cells.

Although a slight delay in tumor growth was observed in most of the combinations of tumor cells and chemokines, only CCL19/B16BL6, XCL1/B16BL6, and CCL22/OV-HM cells demonstrated a notable tumor-suppressive activity in immunocompetent mice as compared with the control vector-transfected cells (Fig. 3). In particular, CCL22-transfection was highly efficacious for the repression of OV-HM tumor growth, since complete rejection was observed in 9 of 10 mice. Furthermore, five of six cured mice could resist rechallenge with parental OV-HM cells, indicating the generation of a long-term tumor-specific immunity by rejection of CCL22/OV-HM cells. CCL22 exhibits a strong chemoattractant activity for a variety of immune cells including T cells, NK cells, and DCs. Guo et al. [28] also reported that the intratumoral injection of conventional Ad encoding human CCL22 resulted in a marked tumor regression in a murine 3LL lung carcinoma model with significant cytotoxic T lymphocyte (CTL) activity. However, CCL22-transfection did not show an anti-tumor effect in both B16BL6 and CT26 cells, and the chemokine that could demonstrate an obvious suppressive effect common to tumor cells of all three kinds was not found even if the results of CCL27/OV-HM and

CX3CL1/OV-HM cells, which were examined in our previous work [19], were included. In addition, some chemokines such as CCL17, CCL20, CCL21, and CX3CL1 failed to induce a notable suppressive effect against all three kinds of tumors although their chemoattractant activity for immune cells was reported. These complicated phenomena suggest that the anti-tumor effect via chemokine expression might be affected by several factors, for example, (1) the immunogenicity of the tumor cells, (2) the quantity and population ratio of the immune cells accumulated in tumor tissue, and (3) the activation state and deviation of the immune system in host.

We considered that not only the accumulation but also the activation of immune cells in tumor tissue is very important in cancer immunotherapy using chemokines, because several approaches that combined chemokines with cytokines or costimulatory molecules resulted in the synergic enhancement of anti-tumor activity as compared with the application of chemokine alone [29–32]. DCs, unique antigen-presenting cells capable of priming and stimulating naive T cells, not only play a critical role in establishing antigen-specific adaptive immune responses but also regulate the innate immune system [33–35]. Because of these properties, DCs loaded with tumor-associated antigen are ideal for generating a primary immune response against cancer as “nature’s adjuvant” [33,36]. We previously reported that the vaccination of DCs transfected with gene coding gp100, one of the melanoma-associated antigens, by AdRGD could induce anti-B16BL6 tumor immunity based on increasing cytotoxic activities of NK cells and gp100-specific CTLs [21]. When chemokine-transfected B16BL6 cells were inoculated into mice vaccinated with gp100-expressing DCs, CCL17, CCL19, CCL22, and CCL27 could promote resistance to tumor formation (Fig. 4). Upon comparing the outcomes in Figs. 3A and 4, CCL19 demonstrated B16BL6 tumor-suppressive activity in both intact and gp100-primed mice, whereas the enhancement of the anti-tumor effect by CCL17, CCL22, or CCL27 was observed only in gp100-primed mice. Surprisingly, the anti-tumor activity of XCL1 detected in intact mice was lost in gp100-primed mice, and the CX3CL1/B16BL6 tumor grew more rapidly than the control tumor in gp100-primed mice. We speculated that the weak anti-B16BL6 tumor activity of XCL1 or CX3CL1 was masked by vaccine efficacy of gp100-expressing DCs, and that the angiogenic activity of CX3CL1 [37] might be emphasized in a tumor-specifically sensitized host.

Collectively, our data suggested that the tumor-suppressive activity of chemokine was greatly influenced by the kind of tumors and the activation state of the immune cells, and that a search for an effective chemokine for cancer immunotherapy should be performed in an experimental model that can reflect clinical status, in-

cluding the immunogenicity of tumors, the state of the host’s immune system, and the combination of other treatments, as much as possible.

Acknowledgments

We are grateful to Dr. Nicholas P. Restifo (National Cancer Institute, Bethesda, MD, USA) for providing the CT26 cells, and to Dr. Hiromi Fujiwara (School of Medicine, Osaka University, Osaka, Japan) for providing the OV-HM cells. This study was supported in part by the Research on Health Sciences focusing on Drug Innovation from The Japan Health Sciences Foundation; by grants from the Bioventure Development Program of the Ministry of Education, Culture, Sports, Science and Technology of Japan; by the Science Research Promotion Fund of the Japan Private School Promotion Foundation; by Grants-in-Aid for Scientific Research (C) from the Ministry of Education, Culture, Sports, Science and Technology of Japan; and by grants from the Ministry of Health and Welfare in Japan.

References

- [1] A. Zlotnik, O. Yoshie, Chemokines: a new classification system and their role in immunity, *Immunity* 12 (2000) 121–127.
- [2] O. Yoshie, T. Imai, H. Nomiya, Chemokines in immunity, *Adv. Immunol.* 78 (2001) 57–110.
- [3] B. Homey, A. Muller, A. Zlotnik, Chemokines: agents for the immunotherapy of cancer?, *Nat. Rev. Immunol.* 2 (2002) 175–184.
- [4] S. Sharma, M. Stolina, J. Luo, R.M. Strieter, M. Burdick, L.X. Zhu, R.K. Batra, S.M. Dubinett, Secondary lymphoid tissue chemokine mediates T cell-dependent antitumor responses in vivo, *J. Immunol.* 164 (2000) 4558–4563.
- [5] T. Fushimi, A. Kojima, M.A. Moore, R.G. Crystal, Macrophage inflammatory protein 3 α transgene attracts dendritic cells to established murine tumors and suppresses tumor growth, *J. Clin. Invest.* 105 (2000) 1383–1393.
- [6] S.E. Braun, K. Chen, R.G. Foster, C.H. Kim, R. Hromas, M.H. Kaplan, H.E. Broxmeyer, K. Cornetta, The CC chemokine CK β -11/MIP-3 β /ELC/Exodus 3 mediates tumor rejection of murine breast cancer cells through NK cells, *J. Immunol.* 164 (2000) 4025–4031.
- [7] T. Miyata, S. Yamamoto, K. Sakamoto, R. Morishita, Y. Kaneda, Novel immunotherapy for peritoneal dissemination of murine colon cancer with macrophage inflammatory protein-1 β mediated by a tumor-specific vector, HVJ cationic liposomes, *Cancer Gene Ther.* 8 (2001) 852–860.
- [8] J. Guo, M. Zhang, B. Wang, Z. Yuan, Z. Guo, T. Chen, Y. Yu, Z. Qin, X. Cao, Fractalkine transgene induces T-cell-dependent antitumor immunity through chemoattraction and activation of dendritic cells, *Int. J. Cancer* 103 (2003) 212–220.
- [9] K.F. Kozarsky, J.M. Wilson, Gene therapy: adenovirus vectors, *Curr. Opin. Genet. Dev.* 3 (1993) 499–503.
- [10] M.A. Kay, S.L. Woo, Gene therapy for metabolic disorders, *Trends Genet.* 19 (1994) 253–257.
- [11] H. Mizuguchi, N. Koizumi, T. Hosono, N. Utoguchi, Y. Watanabe, M.A. Kay, T. Hayakawa, A simplified system for constructing recombinant adenoviral vectors containing heterologous peptides in the HI loop of their fiber knob, *Gene Ther.* 8 (2001) 730–735.
- [12] N. Koizumi, H. Mizuguchi, T. Hosono, A. Ishii-Watabe, E. Uchida, N. Utoguchi, Y. Watanabe, T. Hayakawa, Efficient gene transfer by fiber-mutant adenoviral vectors containing RGD peptide, *Biochim. Biophys. Acta* 1568 (2001) 13–20.

- [13] Y. Okada, N. Okada, S. Nakagawa, H. Mizuguchi, K. Takahashi, N. Mizuno, T. Fujita, A. Yamamoto, T. Hayakawa, T. Mayumi, Tumor necrosis factor α -gene therapy for an established murine melanoma using RGD (Arg-Gly-Asp) fiber-mutant adenovirus vectors, *Jpn. J. Cancer Res.* 93 (2002) 436–444.
- [14] H. Nomiya, K. Hieshima, T. Nakayama, T. Sakaguchi, R. Fujisawa, S. Tanase, H. Nishiura, K. Matsuno, H. Takamori, Y. Tabira, T. Yamamoto, R. Miura, O. Yoshie, Human CC chemokine liver-expressed chemokine/CCL16 is a functional ligand for CCR1, CCR2 and CCR5, and constitutively expressed by hepatocytes, *Int. Immunol.* 13 (2001) 1021–1029.
- [15] H. Mizuguchi, M.A. Kay, Efficient construction of a recombinant adenovirus vector by an improved in vitro ligation method, *Hum. Gene Ther.* 9 (1998) 2577–2583.
- [16] H. Mizuguchi, M.A. Kay, A simple method for constructing E1- and E1/E4-deleted recombinant adenoviral vectors, *Hum. Gene Ther.* 10 (1999) 2013–2017.
- [17] N. Okada, Y. Tsukada, S. Nakagawa, H. Mizuguchi, K. Mori, T. Saito, T. Fujita, A. Yamamoto, T. Hayakawa, T. Mayumi, Efficient gene delivery into dendritic cells by fiber-mutant adenovirus vectors, *Biochem. Biophys. Res. Commun.* 282 (2001) 173–179.
- [18] N. Okada, Y. Masunaga, Y. Okada, S. Iiyama, N. Mori, T. Tsuda, A. Matsubara, H. Mizuguchi, T. Hayakawa, T. Fujita, A. Yamamoto, Gene transduction efficiency and maturation status in mouse bone marrow-derived dendritic cells infected with conventional or RGD fiber-mutant adenovirus vectors, *Cancer Gene Ther.* 10 (2003) 421–431.
- [19] J.Q. Gao, Y. Tsuda, K. Katayama, T. Nakayama, Y. Hatanaka, Y. Tani, H. Mizuguchi, T. Hayakawa, O. Yoshie, Y. Tsutsumi, T. Mayumi, S. Nakagawa, Antitumor effect by interleukin-11 receptor α -locus chemokine/CCL27, introduced into tumor cells through a recombinant adenovirus vector, *Cancer Res.* 63 (2003) 4420–4425.
- [20] P. Janik, P. Briand, N.R. Hartmann, The effect of estrone-progesterone treatment on cell proliferation kinetics of hormone-dependent GR mouse mammary tumours, *Cancer Res.* 35 (1975) 3698–3704.
- [21] N. Okada, Y. Masunaga, Y. Okada, H. Mizuguchi, S. Iiyama, N. Mori, A. Sasaki, S. Nakagawa, T. Mayumi, T. Hayakawa, T. Fujita, A. Yamamoto, Dendritic cells transduced with gp100 gene by RGD fiber-mutant adenovirus vectors are highly efficacious in generating anti-B16BL6 melanoma immunity in mice, *Gene Ther.* 10 (2003) 1891–1902.
- [22] F. Paillard, Cytokine and chemokine: a stimulating couple, *Hum. Gene Ther.* 10 (1999) 695–696.
- [23] J. Laning, H. Kawasaki, E. Tanaka, Y. Luo, M.E. Dorf, Inhibition of in vivo tumor growth by the β chemokine, TCA3, *J. Immunol.* 153 (1994) 4625–4635.
- [24] K. Hirose, M. Hakozi, Y. Nyunoya, Y. Kobayashi, K. Matsushita, T. Takenouchi, A. Mikata, N. Mukaida, K. Matsushima, Chemokine gene transfection into tumour cells reduced tumorigenicity in nude mice in association with neutrophilic infiltration, *Br. J. Cancer* 72 (1995) 708–714.
- [25] J.J. Mule, M. Custer, B. Averbook, J.C. Yang, J.S. Weber, D.V. Goeddel, S.A. Rosenberg, T.J. Schall, RANTES secretion by gene-modified tumor cells results in loss of tumorigenicity in vivo: role of immune cell subpopulations, *Hum. Gene Ther.* 7 (1996) 1545–1553.
- [26] E. Nakashima, A. Oya, Y. Kubota, N. Kanada, R. Matsushita, K. Takeda, F. Ichimura, K. Kuno, N. Mukaida, K. Hirose, I. Nakanishi, T. Ujiie, K. Matsushima, A candidate for cancer gene therapy: MIP-1 α gene transfer to an adenocarcinoma cell line reduced tumorigenicity and induced protective immunity in immunocompetent mice, *Pharm. Res.* 13 (1996) 1896–1901.
- [27] M. Maric, Y. Liu, Strong cytotoxic T lymphocyte responses to a macrophage inflammatory protein 1 α -expressing tumor: linkage between inflammation and specific immunity, *Cancer Res.* 59 (1999) 5549–5553.
- [28] J. Guo, B. Wang, M. Zhang, T. Chen, Y. Yu, E. Regulier, H.E. Homann, Z. Qin, D.W. Ju, X. Cao, Macrophage-derived chemokine gene transfer results in tumor regression in murine lung carcinoma model through efficient induction of antitumor immunity, *Gene Ther.* 9 (2002) 793–803.
- [29] P.C. Emtage, Y. Wan, M. Hitt, F.L. Graham, W.J. Muller, A. Zlotnik, J. Gauldie, Adenoviral vectors expressing lymphotactin and interleukin 2 or lymphotactin and interleukin 12 synergize to facilitate tumor regression in murine breast cancer models, *Hum. Gene Ther.* 10 (1999) 697–709.
- [30] I. Narvaiza, G. Mazzolini, M. Barajas, M. Duarte, M. Zaratiegui, C. Qian, I. Melero, J. Prieto, Intratumoral coinjection of two adenoviruses, one encoding the chemokine IFN- γ -inducible protein-10 and another encoding IL-12, results in marked antitumoral synergy, *J. Immunol.* 164 (2000) 3112–3122.
- [31] J.M. Ruehlmann, R. Xiang, A.G. Niethammer, Y. Ba, U. Pertl, C.S. Dolman, S.D. Gillies, R.A. Reisfeld, MIG (CXCL9) chemokine gene therapy combines with antibody-cytokine fusion protein to suppress growth and dissemination of murine colon carcinoma, *Cancer Res.* 61 (2001) 8498–8503.
- [32] K.A. Tolba, W.J. Bowers, J. Muller, V. Houseknecht, R.E. Giuliano, H.J. Federoff, J.D. Rosenblatt, Herpes simplex virus (HSV) amplicon-mediated codelivery of secondary lymphoid tissue chemokine and CD40L results in augmented antitumor activity, *Cancer Res.* 62 (2002) 6545–6551.
- [33] R.M. Steinman, Dendritic cells and immune-based therapies, *Exp. Hematol.* 24 (1996) 859–862.
- [34] J. Banchereau, R.M. Steinman, Dendritic cells and the control of immunity, *Nature* 392 (1998) 245–252.
- [35] F. Granucci, I. Zanoni, S. Feau, P. Ricciardi-Castagnoli, Dendritic cell regulation of immune responses: a new role for interleukin 2 at the intersection of innate and adaptive immunity, *EMBO J.* 22 (2003) 2546–2551.
- [36] L. Fong, E.G. Engleman, Dendritic cells in cancer immunotherapy, *Annu. Rev. Immunol.* 18 (2000) 245–273.
- [37] M.V. Volin, J.M. Woods, M.A. Amin, M.A. Connors, L.A. Harlow, A.E. Koch, Fractalkine: a novel angiogenic chemokine in rheumatoid arthritis, *Am. J. Pathol.* 159 (2001) 1521–1530.

Department of Biopharmaceutics¹, Graduate School of Pharmaceutical Sciences, Osaka University, Japan, Department of Pharmaceutics², School of Pharmaceutical Sciences, Zhejiang University, P.R. China, Division of Cellular and Gene Therapy Products³, National Institute of Health Sciences, Japan, Department of Microbiology⁴, Kinki University School of Medicine, Japan

Tumor-suppressive activities by chemokines introduced into OV-HM cells using fiber-mutant adenovirus vectors

J.Q. GAO^{1,2}, L.S. ALEXANDRE¹, Y. TSUDA¹, K. KATAYAMA¹, Y. ETO¹, F. SEKIGUCHI¹, H. MIZUGUCHI³, T. HAYAKAWA³, T. NAKAYAMA⁴, O. YOSHIE⁴, Y. TSUTSUMI¹, T. MAYUMI¹, S. NAKAGAWA¹

Received September 11, 2003, accepted September 19, 2003

Shinsaku Nakagawa, Ph.D., Department of Biopharmaceutics, Graduate School of Pharmaceutical Sciences, Osaka University, Yamadaoka 1-6, 565-0871 Suita City, Osaka, Japan
nakagawa@phs.osaka-u.ac.jp

Pharmazie 59: 238–239 (2004)

In this study, fiber-mutant adenovirus vectors encoding chemokines, Ad-RGD-mCCL17, Ad-RGD-mCCL21 and Ad-RGD-mCCL22 were constructed. The insertion of integrin-targeting RGD sequence into fiber knob of adenovirus vectors notably enhanced the infection efficiency into tumor cells. Among three chemokine-encoding vectors evaluated, Ad-RGD-mCCL22 showed significant tumor-suppressive activity via transduction into OV-HM cells.

Cytokine or chemokine encoded by a viral vector is currently regarded as a promising way of cancer gene immunotherapy. Chemokines consist of a superfamily of small secreted proteins that attract their target cells by interacting with G protein-coupled receptors expressed on these cells. Researchers have paid attention to chemotactic activity of chemokines for immune cells, and have expected that they may be able to play a pivotal role in cancer treatment, because the basis and premise of immunotherapy is the accumulation of immune cells in tumor tissues. More than 40 chemokines have been identified so far (Yoshie et al. 2001), but only a few have been demonstrated as candidates for cancer therapy by using as sole agents or with adjuvant (Gao et al. 2003; Maric and Liu 1999).

In the present report, three CC family chemokines, thymus and activation-regulated chemokine/CCL17, secondary lymphoid-tissue chemokine/CCL21 and macrophage-derived chemokine/CCL22 have been studied. CCL17 and CCL22 are chemotactic for memory CD4⁺ T cells via CCR4 while CCL21 induces migration of T cells, B cells, dendritic cells and NK cells via CCR7 (Campbell et al. 1999, Nagira et al. 1997). CCL22 was also shown to have a chemoattractant activity for dendritic cells, NK cells and T cells (Godiska et al. 1997). We hypothesized that if tumor cells could be genetically modified *in vitro* to produce chemokines *in vivo*, the chemokines would accumulate immune cells in the tumor. The facilitated interaction of immune cells with the tumor cells *in vivo* might induce

Table: EGFP expression in OV-HM cells infected with Ad-EGFP and Ad-RGD-EGFP

	250 PT % gated	500 PT % gated
Non-infection	0.94%	0.94%
Ad-EGFP	47.1%	76.3%
Ad-RGD-EGFP	98.7%	99.6%

OV-HM cells were infected with 250 or 500 particles/cell of Ad-EGFP or Ad-RGD-EGFP for 48 h and EGFP expression was measured by flow cytometric analysis

anti-tumor activity. To test this hypothesis, we developed a recombinant adenovirus vector with a fiber mutation containing the integrin-targeting Arg-Gly-Asp (RGD) sequence in the fiber knob (Mizuguchi et al. 2001b). As shown in the Table, This vector has been demonstrated to possess higher transduction efficacy to OV-HM cells, a mouse ovary carcinoma line (Hashimoto et al. 1989), compared to that of conventional adenovirus vector.

In this study, we infected OV-HM with fiber-mutant adenovirus vectors encoding mCCL17, mCCL21 or mCCL22 and examined their expression by RT-PCR. The migration assay of chemokine-encoding vectors was also conducted *in vitro*. The results demonstrated that the efficient production of biologically active mCCL17, mCCL21 and mCCL22 could be detected in the culture supernatants of cells infected with these vectors, and the vectors could efficiently migrate the specific receptor-expressing cells (data not shown). Then OV-HM cells infected with Ad-RGD-mCCL17, Ad-RGD-mCCL21, Ad-RGD-mCCL22 or Ad-RGD-NULL (the control vector only) were intradermally inoculated into B6C3F1 mice to evaluate their effects on tumor growth *in vivo*. As shown in the Fig., OV-HM infected with Ad-RGD-mCCL22 showed significant suppression in tumor growth. On the other hand, OV-HM infected with either Ad-RGD-mCCL17 or Ad-RGD-mCCL21 did not show any difference in tumor growth from that infected with Ad-RGD-NULL. In rechallenge experiment, mice that had complete regression were intradermally injected with OV-HM or B16/BL6 cells 90 days after the initial challenge. Results demonstrated that 100% of mice rechallenged with OV-HM remained tumor-free. In contrast, all of the mice rechallenged with B16/BL6 developed palpable tumors within 2 weeks (data not shown). These results indicated the generation of specific immunity against OV-HM in mice that rejected OV-HM expressing mCCL22. To exclude the possibility that the growth suppression of the tumor cells by Ad-RGD-mCCL22 was due to the cytotoxicity of adenovirus or

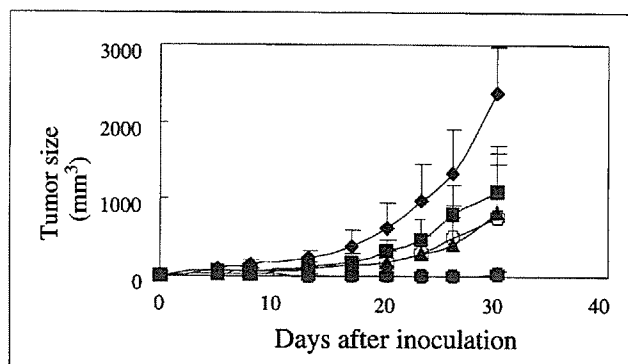


Fig.: Tumor-suppressive activity of Ad-RGD-mCCL22
◆—No-treat, ■—Ad-RGD-NULL, ▲—Ad-RGD-mCCL17,
●—Ad-RGD-mCCL22, ○—Ad-RGD-mCCL21

chemokine, OV-HM cells transfected with Ad-RGD-mCCL17, Ad-RGD-mCCL21, Ad-RGD-mCCL22 or Ad-RGD-NULL were cultured for 48 h, and the cell viability was measured by the MTT assay. The *in vitro* growth of the cells infected with these vectors was essentially identical to that of control cells (data not shown).

In summary, our study suggests that CCL22, a CC family chemokine, may be a good candidate for cancer gene immunotherapy.

Experimental

1. Cell lines and animals

OV-HM ovarian carcinoma cells were kindly provided by Dr. Hiromi Fujiwara (School of Medicine, Osaka University, Japan) and were maintained in RPMI 1640 supplemented with 10% heat-inactivated FBS. Human embryonic kidney (HEK) 293 cells were cultured in DMEM supplemented with 10% FBS. All the cell lines were cultured at 37 °C in a humidified atmosphere with 5% CO₂. Female B6C3F1 mice (6–8 week of age) were purchased from SLC Inc. (Hamamatsu, Japan). All of the experimental procedures were in accordance with the Osaka University guidelines for the welfare of animals in experimental neoplasia.

2. Procedures

2.1. Infection of chemokines into OV-HM cells using fiber-mutant adenovirus vectors

Replication-deficient adenovirus vectors used in this study were based on the adenovirus serotype 5 backbone with deletions of E1 and E3 and the expression cassette in the E1 region (Mizuguchi et al. 2001a). The integrin-targeting RGD sequence was inserted into the HI loop of the fiber knob using a two-step method (Mizuguchi et al. 2001b). Fiber-mutant adenovirus vectors, Ad-RGD-mCCL17, Ad-RGD-mCCL21 and Ad-RGD-mCCL22 carrying the murine chemokine cDNA under the control of the cytomegalovirus promoter, were constructed by an improved *in vitro* ligation method as described (Mizuguchi and Kay 1998). The Ad-RGD-NULL vector, serving as a negative control, is identical to the Ad-RGD-chemokine vectors without the chemokine gene in the expression cassette. The adenovirus vectors were propagated in HEK 293 cells and purified by cesium chloride gradient ultracentrifugation, and their titer was determined by plaque-forming assay.

2.2. Tumor rejection in mice and subsequent rechallenge by tumor reinoculation

1×10^6 OV-HM cells that had been infected with Ad-RGD-mCCL17, Ad-RGD-mCCL21 or Ad-RGD-mCCL22 at a MOI (Multiplicity of Infection) of 10 for 24 h were inoculated intradermally into the flank of mice. The length and width of the tumor were measured twice a week. Animals were euthanized when one of the two measurements were greater than 15 mm. Three months after complete regression of primary tumors, mice were rechallenged with freshly isolated OV-HM tumor cells or B16/BL6 melanoma cells by intradermal injection of 1×10^6 cells into the flank.

References

- Campbell JJ, Haraldsen G, Pan J et al. (1999) The chemokine receptor CCR4 in vascular recognition by cutaneous but not intestinal memory T cells. *Nature* 400: 776–780.
- Gao JQ, Tsuda Y, Katayama K et al. (2003) Anti-tumor effect by interleukin-11 receptor alpha-locus chemokine/CCL27, introduced into tumor cells through a recombinant adenovirus vector. *Cancer Res* 63: 4420–4425.
- Godiska R, Chantry D, Raport CJ et al. (1997) Human macrophage-derived chemokine (MDC), a novel chemoattractant for monocytes, monocyte-derived dendritic cells, and natural killer cells. *J Exp Med* 185: 1595–1604.
- Hashimoto M, Niwa O, Nitta Y et al. (1989) Unstable expression of E-Cadherin adhesion molecules in metastatic ovarian tumor cells. *Jpn J Cancer Res* 80: 459–463.
- Maric M, Liu Y (1999) Strong cytotoxic T lymphocyte responses to a macrophage inflammatory protein 1 alpha-expressing tumor: linkage between inflammation and specific immunity. *Cancer Res* 59: 5549–5553.
- Mizuguchi H, Kay MA, Hayakawa T (2001a) *In vitro* ligation-based cloning of foreign DNAs into the E3 and E1 deletion regions for generation of recombinant adenovirus vectors. *Biotechniques* 30: 1112–1114.
- Mizuguchi H, Koizumi N, Hosono T et al. (2001b) A simplified system for constructing recombinant adenoviral vectors containing heterologous peptides in the HI loop of their fiber knob. *Gene Ther* 8: 730–735.

Mizuguchi H, Kay MA (1998) Efficient construction of a recombinant adenovirus vector by an improved *in vitro* ligation method. *Hum Gene Ther* 9: 2577–2583.

Nagira M, Imai T, Hieshima K et al. (1997) Molecular cloning of a novel human CC chemokine secondary lymphoid-tissue chemokine that is a potent chemoattractant for lymphocytes and mapped to chromosome 9p13. *J Biol Chem* 272: 19518–19524.

Yoshie O, Imai T, Nomiyama H (2001) Chemokines in immunity. *Adv Immunol* 78: 57–110.

RNA interfering approach for clarifying the PPAR γ pathway using lentiviral vector expressing short hairpin RNA

Kazufumi Katayama^a, Koichiro Wada^{b,*}, Hiroyuki Miyoshi^c, Kozo Ohashi^a, Masashi Tachibana^a, Rie Furuki^a, Hiroyuki Mizuguchi^d, Takao Hayakawa^d, Atsushi Nakajima^e, Takashi Kadowaki^f, Yasuo Tsutsumi^a, Shinsaku Nakagawa^a, Yoshinori Kamisaki^b, Tadanori Mayumi^a

^aDepartment of Biopharmaceutics, Graduate School of Pharmaceutical Science, Osaka University, Osaka 565-0871, Japan

^bDepartment of Pharmacology, Graduate School of Dentistry, Osaka University, 1-8 Yamadaoka, Suita, Osaka 565-0871, Japan

^cSubteam for Manipulation of Cell Fate, BioResource Center, RIKEN, Tsukuba Institute, Ibaraki, Japan

^dDivision of Biological Chemistry and Biologicals, National Institute of Health Sciences, Tokyo 158-8501, Japan

^eThe Third Department of Internal Medicine, Yokohama City University School of Medicine, Yokohama 236-0004, Japan

^fDepartment of Metabolic Diseases, Graduate School of Medicine, University of Tokyo, Tokyo, 113-0033, Japan

Received 15 December 2003; revised 10 January 2004; accepted 22 January 2004

First published online 4 February 2004

Edited by Robert Barouki

Abstract Peroxisome proliferator-activated receptor γ (PPAR γ) plays a central role in adipocyte differentiation and insulin sensitivity. Although PPAR γ also appears to regulate diverse cellular processes in other cell types such as lymphocytes, the detailed mechanisms remain unclear. In this study, we established a lentivirus-mediated short hairpin RNA expression system and identified a potent short hairpin RNA which suppresses PPAR γ expression, resulting in marked inhibition of preadipocyte-to-adipocyte differentiation in 3T3-L1 cells. Our PPAR γ -knock-down method will serve to clarify the PPAR γ pathway in various cell types *in vivo* and *in vitro*, and will facilitate the development of therapeutic applications for a variety of diseases.

© 2004 Federation of European Biochemical Societies. Published by Elsevier B.V. All rights reserved.

Key words: Peroxisome proliferator-activated receptor γ ; RNA interference; Short hairpin RNA; Lentiviral vector; Adipocyte

1. Introduction

The peroxisome proliferator-activated receptor (PPAR) family was discovered as an orphan nuclear receptor, and three different subtypes were subsequently identified, namely PPAR α , PPAR δ/β and PPAR γ . PPAR γ is abundantly expressed in adipose tissue and plays a key role in adipocyte differentiation and insulin sensitivity [1]. Recently, our group and other researchers reported that PPAR γ is also an attractive therapeutic target as it can play an important role in immune responses, especially in transcriptional regulation of inflammatory responses [2–5].

The biological role of PPAR γ had been widely investigated by using PPAR γ -deficient mice generated by targeted disruption

of the PPAR γ gene. Since homozygous PPAR γ -deficient mice (PPAR $\gamma^{-/-}$) are embryonic lethal due to placental dysfunction [1], heterozygous mice (PPAR $\gamma^{+/-}$) have been used to investigate the role of PPAR γ *in vivo* experiments. However, PPAR $\gamma^{+/-}$ mice seem to be of limited use in some experiments, because PPAR γ also appears to regulate diverse cellular processes in cells that show lower levels of PPAR γ expression in comparison to adipose tissue [6,7].

RNA interference (RNAi) is a powerful technique for selectively silencing the expression of genes. Recent work has provided a system for the stable expression of short interfering RNA (siRNA) in mammalian cells, which is generally based on the expression of short hairpin RNA (shRNA) under the control of the RNA polymerase III promoter [8–11]. The technique has allowed for the development of a new approach for achieving targeted gene silencing of disease-associated genes in animal models as well as in cultured cells.

Lentiviral vectors (LVs) are a promising tool for exogenous gene transfer among gene transfer vehicles, because LVs have the advantages of infecting non-dividing cells and being stably integrated into the host genome resulting in long-term expression of transgene [12–16]. Furthermore, recent reports have demonstrated that virus-mediated RNAi could provide long-term silencing in mammalian cells [9,17,18]. In the present study, we attempted to develop a technique for suppressing the expression of PPAR γ *in vivo* and *in vitro*. We established a lentivirus-mediated shRNA expression system and identified a potent shRNA target sequence in the coding region of PPAR γ mRNA. This approach has enabled us to clarify a novel role of PPAR γ .

2. Materials and methods

2.1. Vector construction

Vectors were constructed using standard cloning procedures. HI-RNA promoter was amplified from human genomic DNA (Clontech, Palo Alto, CA, USA) using the following primers: 5'-CCATGGAATTGCAACGCTGACGTC-3' and 5'-GCAAGCTTAGATCTGTGGTCTCATAAGAACTTATAAGATTCCC-3'. The amplified polymerase chain reaction (PCR) product was inserted into the *EcoRI*-*Bgl*II site of pHM5 [19], generating pHM5-H1. pHM5-H1 was designed to express shRNA upon the insertion of an appropriate sequence into the *Bgl*II/*Xba*I site (Fig. 1A). Oligonucleotides encoding

*Corresponding author. Fax: (81)-6-6879 2914.

E-mail address: kwada@dent.osaka-u.ac.jp (K. Wada).

Abbreviations: LV, lentiviral vector; shRNA, short hairpin RNA; MOI, multiplicity of infection; PPAR, peroxisome proliferator-activated receptor; GPDH, glycerol-3-phosphate dehydrogenase; BRL, rosiglitazone (BRL-49653)

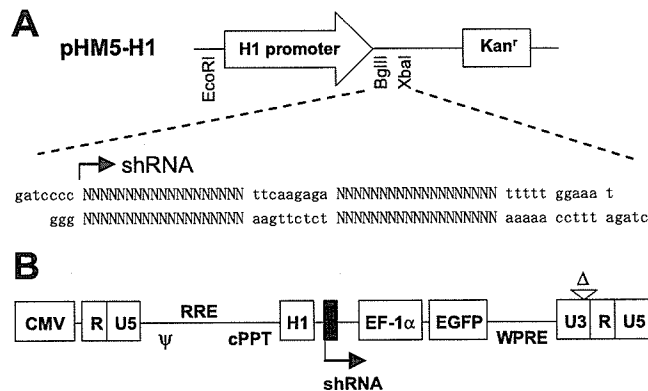


Fig. 1. Vector construction. A: pHM5-H1 was constructed as described in Section 2. Oligonucleotides encoding both strands of the targeting sequence, a spacer sequence which provided a loop structure and a transcriptional termination signal T5 were annealed and inserted into *Bgl*III/*Xba*I sites in pHM5-H1. B: Schematic representation of self-inactivating (SIN) LV plasmid (CS-H1-shRNA-EG). CMV: cytomegalovirus promoter, Ψ: packaging signal, RRE: rev responsive element, cPPT: central polypurine tract, H1: human H1 promoter, EF-1α: human elongation factor 1α subunit gene promoter, EGFP: enhanced green fluorescent protein, WPRE: woodchuck hepatitis virus posttranscriptional regulatory element. Δ: deleting 133 bp in the U3 region of the 3' long terminal repeat.

both strands of the targeting sequence were annealed and inserted into *Bgl*III/*Xba*I sites of pHM5-H1 (Fig. 1A and Table 1). The sequence was verified on a DNA sequencer (ABI Prism 310, Applied Biosystems) and the cassette containing the H1 promoter plus the shRNA was transferred to a self-inactivating (SIN) LV construct, generating CS-H1-shRNA-EG (Fig. 1B).

2.2. Preparation of LV expressing shRNA (LV-shRNA)

LVs pseudotyped with vesicular stomatitis virus G glycoprotein (VSV-G) were prepared according to a previously described method [15,20,21]. Briefly, 293T cells were transfected with four plasmids: packaging construct (pMDLg/pRRE), VSV-G-expressing construct (pMD.G), Rev-expressing construct (pRSV-Rev), and SIN vector construct (CS-H1-shRNA-EG). Vector supernatant was concentrated by ultracentrifugation, and the pellet was resuspended in Hanks' balanced salt solution. Vector titers, which can be detected by enhanced green fluorescent protein (EGFP) expression under the control of a human elongation factor 1α subunit gene promoter, were determined by infection of HeLa P4 cells with serial dilutions of the vector stocks, followed by fluorescence-activated cell sorter (FACS) analysis for EGFP-positive cells.

2.3. Cell culture and infection of LV-shRNA

3T3-L1 preadipocytes were cultured in Dulbecco's modified Eagle's medium supplemented with 10% fetal bovine serum. The 3T3-L1 cells were infected with viral stocks at a multiplicity of infection (MOI) of 50 or 200, followed by FACS analysis for EGFP expression. Transduction efficiencies were $66.57\% \pm 1.44$ at 50 MOI and $91.64\% \pm 1.07$ at 200 MOI, expressed as S.E.M. The transduced 3T3-L1 cells were grown and then used in subsequent experiments.

2.4. Differentiation protocol

Induction of adipocyte differentiation was performed essentially as described [22]. Two days after confluence (day 0), the medium was replaced with differentiation medium containing rosiglitazone (BRL, 1 μM), insulin (INS, 150 nM), dexamethasone (DEX, 1 μM) and 3-isobutyl-1-methylxanthine (IBMX, 100 μM), which was changed every 3 days thereafter until analysis.

2.5. Measurement of adipocyte differentiation

Differentiation of 3T3-L1 preadipocytes to adipocytes was monitored by measurement of intracellular lipid accumulation using Oil red O staining and glycerol-3-phosphate dehydrogenase (GPDH) ac-

tivity on day 9. Cultured cells were fixed for 2 h with 10% formalin in isotonic phosphate buffer and then washed with distilled water. The cells were then stained by complete immersion in a working solution (0.3%) of Oil red O for 4 h. Excess dye was removed by exhaustive washing with water. The GPDH activity was measured using a GPDH assay kit (Hokudo, Hokkaido, Japan).

2.6. RNA isolation and reverse transcription (RT) PCR analysis

Total RNA was extracted from the 3T3-L1 cells infected with each kind of LV-shRNA using Tri-Reagent (Sigma). First-strand cDNA was generated from 1 μg of RNA by using oligo(dT)₁₂₋₁₈ primer (Invitrogen) and SuperScript III RNase H Reverse Transcriptase (Invitrogen) according to the manufacturer's protocol. The reverse transcription reaction mix was amplified with the following pair of oligonucleotides specific for murine PPARα, PPARδ, PPARγ2 and glyceraldehyde-3-phosphate dehydrogenase (GAPDH): PPARα, 5'-CGACAAGTGTGATCGGAGCTGCAAG-3' and 5'-GTTGAAGT-TCTTCAGGTAGGCTTC-3'; PPARδ, 5'-GGCCAACGGCAGTG-GCTTCGTC-3' and 5'-GGCTGCGGCCCTTAGTACATGTCTC-3'; PPARγ2, 5'-GCTGTTATGGGTGAAACTCTG-3' and 5'-ATAA-GGTGGAGATGCAGGTTC-3'; GAPDH, 5'-GCTCACTGGCAT-GGCCTTC-3' and 5'-ACCACCCTGTGCTGTAGC-3' [23]. The sample was amplified in the linear phase, optimized for each gene (PPARα: 38 cycles; PPARδ: 30 cycles; PPARγ2: 36 cycles; GAPDH: 23 cycles). All PCR products were electrophoresed on 2% agarose gel using 0.5×Tris-borate-EDTA buffer and visualized using ethidium bromide. The gel image was captured by a digital camera, and densitometric analysis was performed using NIH Image software.

2.7. Western blot analysis

Cultured cells were homogenized in Tris-HCl buffer containing a cocktail of protease inhibitors and insoluble materials were then removed by centrifugation at 4°C. The solubilized lysates were resolved by sodium dodecyl sulfate-polyacrylamide gel electrophoresis under reducing conditions at a concentration of 5 μg protein of sample per lane. Detection of PPARα, PPARδ, PPARγ and GAPDH was respectively performed with anti-PPARα polyclonal antibody (Santa Cruz Biotechnology, Santa Cruz, CA, USA), anti-PPARδ polyclonal antibody (Santa Cruz Biotechnology), anti-PPARγ monoclonal antibody (Santa Cruz Biotechnology) and anti-GAPDH polyclonal antibody (Trevigen, Gaithersburg, MD, USA) according to a previously described method [4]. The band intensity was quantified using NIH Image software.

2.8. Statistical analysis

All results are expressed as mean ± S.E.M. Statistical comparisons were made with Student's *t*-test or Scheffé's method after analysis of variances. The results were considered significantly different at $P < 0.05$.

Table 1
LV vectors used in this study

LV vector	shRNA target gene	shRNA target sequence
LV-shRNA-P11	PPARγ1 and 2	CAGCTCTACAACAGGCCCTC
LV-shRNA-P12	PPARγ1 and 2	ATGGCCATTGAGTGCCGAG
LV-shRNA-P13	PPARγ1 and 2	TAAATGTCAGTACTGTCCGG
LV-shRNA-P14	PPARγ1 and 2	TTGCCGGAGATCTCCAGTG
LV-shRNA-P15	PPARγ1 and 2	GTCTGCTGATCTGCGAGCC
LV-shRNA-P16	PPARγ1 and 2	TCACCATTGTCTCTACG
LV-shRNA-P17	PPARγ1 and 2	GTTTGAGTTTGCTGTGAAG
LV-shRNA-P18	PPARγ1 and 2	ATGAGCCTTCACCCCTGC
LV-shRNA-P19	PPARγ1 and 2	GATCTGCGAGCCCTGGCAA
LV-shRNA-P21	PPARγ2	ACTCTGGGAGATCTCCTTG
LV-shRNA-P22	PPARγ2	CCTTCGCTGATGCAGTCC
LV-shRNA-Lu	Luciferase	ACGCTGAGACTTCGAAAT
LV-shRNA-Scramble	No target gene	GCGCGCTTTGTAGGATTCG
LV-EG	-	-

LV-EG has no shRNA-expressing cassette. All vectors carry an EGFP-expressing cassette as a marker gene so that the cells transduced with LV-shRNAs can be identified by green fluorescence.

3. Results and discussion

To develop an effective PPAR γ -knockdown method, we constructed an LV-based siRNA system in which shRNA encoding both strands of the targeting sequence is expressed under the control of human H1 promoter [24]. A human H1 promoter was cloned to generate pHM5-H1, and oligonucleotide encoding shRNA against PPAR γ mRNA was inserted (Fig. 1A). Subsequently, the cassette containing the H1 promoter plus the shRNA was transferred to the SIN LV construct (Fig. 1B). Using a shRNA target sequence against firefly luciferase, we previously demonstrated that our LV-based siRNA system effectively suppressed the target gene in mammalian cells (data not shown).

PPAR γ exists as two isoforms, termed PPAR γ 1 and PPAR γ 2,

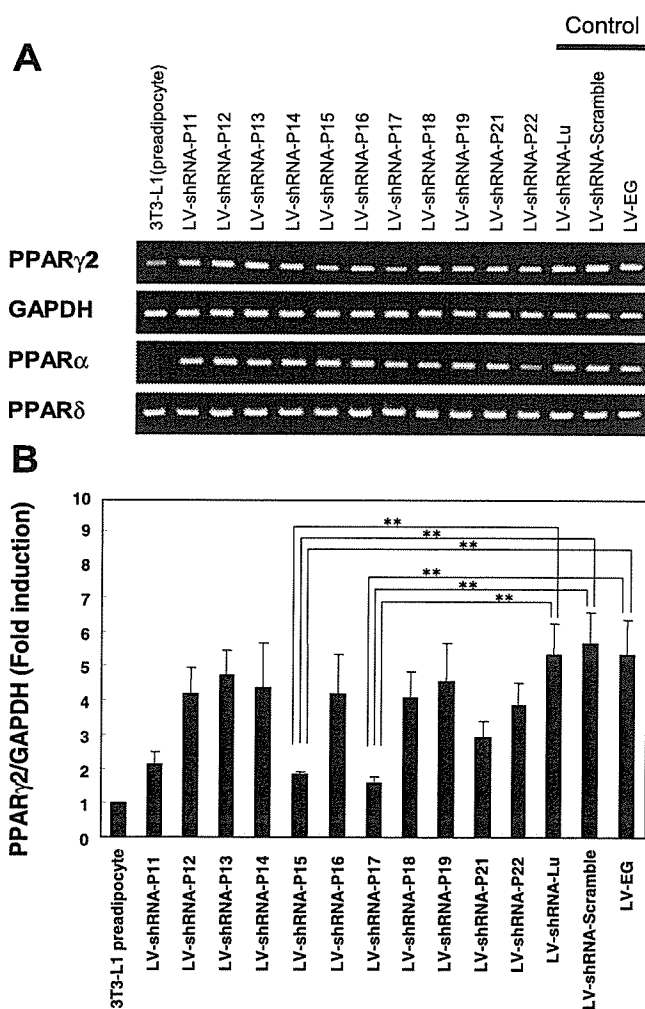


Fig. 2. Alteration of PPAR family mRNA levels in 3T3-L1 cells transduced with LV-shRNAs. A: 3T3-L1 preadipocytes were infected with each LV-shRNA (200 MOI) and then subjected to the differentiation protocol. Two days after the induction of adipocyte differentiation, mRNA levels of PPAR γ 2, PPAR α , PPAR δ , and GAPDH were determined by RT-PCR analysis. Results are representative gel images. B: Densitometric quantitation for PPAR γ and GAPDH from three to four independent experiments. Each PPAR γ value was normalized to the values for GAPDH and expressed as fold induction over the basal level detected in 3T3-L1 preadipocytes (bars, S.E.M.). ** $P < 0.01$ for LV-shRNA-P15 and -P17 compared with LV-shRNA-Lu, LV-shRNA-Scramble or LV-EG.

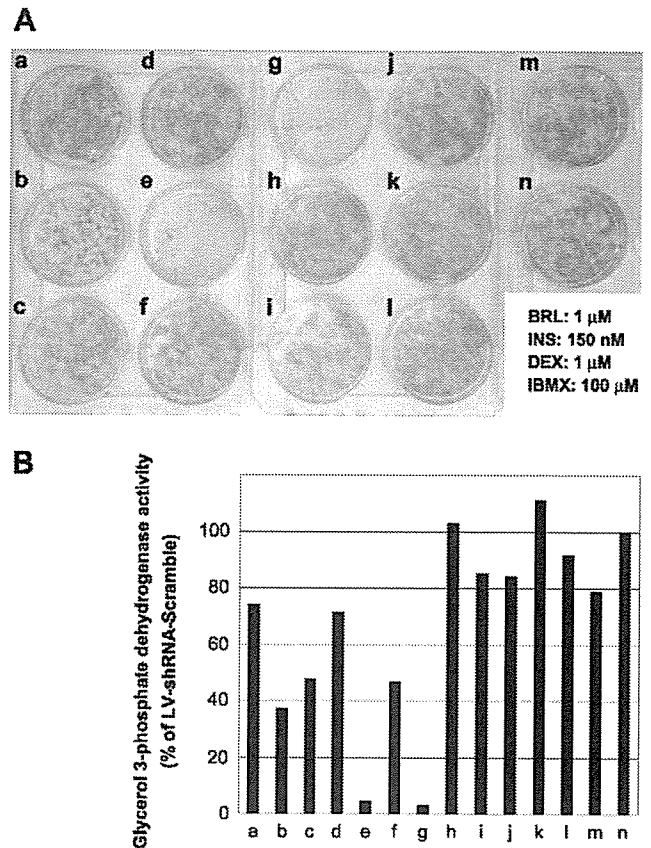


Fig. 3. Effect of LV-shRNAs on adipocyte differentiation. A: Differentiation of 3T3-L1 preadipocytes (infected with LV-shRNA; 200 MOI) to adipocytes was monitored by measurement of intracellular lipid accumulation using Oil red O staining on day 9. B: GPDH activity was measured on day 9. Data were expressed as percentage of the GPDH activity of 3T3-L1 cells which were infected with LV-shRNA-Scramble (200 MOI). a: LV-shRNA-P11; b: LV-shRNA-P12; c: LV-shRNA-P13; d: LV-shRNA-P14; e: LV-shRNA-P15; f: LV-shRNA-P16; g: LV-shRNA-P17; h: LV-shRNA-P18; i: LV-shRNA-P19; j: LV-shRNA-P21; k: LV-shRNA-P22; l: LV-EG; m: LV-shRNA-Lu; n: LV-shRNA-Scramble. Similar results were obtained in two independent experiments.

which are produced by a combination of different promoters and alternative splicing. PPAR γ 2 has an N-terminal extension of 30 amino acids and is very highly expressed in adipocytes [22,25]. We selected 11 target sequences in the coding region of PPAR γ mRNA and constructed LV-shRNAs against PPAR γ (Table 1). In the present study, LV-shRNA-Lu, LV-shRNA-Scramble and LV-EG were used as controls.

To find the most effective shRNA target sequence against PPAR γ , we analyzed the silencing of PPAR γ in 3T3-L1 cells during preadipocyte-to-adipocyte differentiation in which PPAR γ is known to be a master regulator of adipogenesis [1,26,27]. The expression of PPAR γ increases during the differentiation process and activation of PPAR γ protein by its ligand leads to adipogenesis through the activation of the adipogenic gene cascade. The 3T3-L1 preadipocytes transduced with each of the LV-shRNAs, i.e. 3T3-L1 cells expressing shRNAs, as listed in Table 1, were exposed to differentiation medium (DM) 2 days after confluence (day 0). Initially, silencing of PPAR γ expression was examined by RT-PCR after 2 days of culture in DM (Fig. 2). Although 3T3-L1 cells transduced with LV-shRNA-Lu, -Scramble and LV-EG showed

significant increases in the levels of PPAR γ mRNA, 3T3-L1 cells transduced with LV-shRNA-P15 and -P17 retained low levels of PPAR γ mRNA comparable to the level in preadipocytes maintained in normal culture medium. In contrast, the expression levels of GAPDH, PPAR α and PPAR δ were not altered by LV-shRNA-P15 or -P17. The other LV-shRNAs against PPAR γ caused moderate decreases in the levels of PPAR γ mRNA.

The differentiation of 3T3-L1 preadipocytes to adipocytes can be monitored by measurement of intracellular lipid accumulation and GPDH (an important enzyme in triglyceride

synthesis) activity [28–30]. Intracellular lipid accumulation was dramatically reduced in the LV-shRNA-P15- and -P17-infected 3T3-L1 cells as shown by Oil red O staining (Fig. 3A, e: LV-shRNA-P15; g: LV-shRNA-P17). GPDH activity also demonstrated that LV-shRNA-P15 and LV-shRNA-P17 express a potent shRNA which suppresses PPAR γ mRNA expression, resulting in marked inhibition of preadipocyte-to-adipocyte differentiation (Fig. 3B). We also confirmed that the expression of PPAR γ -inducible genes, such as uncoupling protein-1 and adipocyte fatty acid binding protein, were inhibited in 3T3-L1 cells transduced with LV-shRNA-P15 and LV-shRNA-P17 in the presence of the PPAR γ -specific ligand, BRL (unpublished data).

A recent study demonstrated that if the degree of complementarity to its target is reduced, siRNA can function as microRNAs which affect translational suppression without cleavage [31]. An important objective of this study was to determine whether the silencing effect of PPAR γ caused by these LV-shRNAs was specific for PPAR γ . In fact, several shRNA target sequences used in this study partially correspond to PPAR α or PPAR δ . Western blotting analysis demonstrated that PPAR γ protein levels were significantly decreased in the LV-shRNA-P15- and LV-shRNA-P17-infected 3T3-L1 cells, while LV-shRNAs did not alter the amount of PPAR α , PPAR δ or GAPDH protein (Fig. 4). These results were consistent with the result from RT-PCR analysis (Fig. 2).

Furthermore, we examined 3T3-L1 cells exposed to either LV-shRNA-Scramble, -P15 or -P17 by fluorescent microscopy for EGFP expression to identify cells not infected with those vectors, i.e. the 3T3-L1 cells not expressing the shRNA encoded by LV-shRNA-P15 or -P17 (Fig. 5). In the case of LV-shRNA-Scramble, which expresses control shRNA, the differentiation of preadipocytes to adipocytes was not affected by infection with LV. In contrast, all of the cells infected with LV-shRNA-P15 or -P17 retained their fibroblast-like morphology. Taken together, these results indicate that our LV-shRNA-based PPAR γ -knockdown method resulted in decreased PPAR γ expression and specific inhibition of the PPAR γ pathway, even in the case of adipocyte differentiation in which PPAR γ expression is strongly induced by DM and PPAR γ protein is effectively activated by the PPAR γ -specific ligand used in this study, BRL.

Accessibility of the siRNA might depend on the secondary structure of the target mRNA. However, a clear correlation between either secondary structure or GC content and effectiveness of target sites has not yet been recognized. Although we designed 11 different shRNAs against PPAR γ , we have not found any correlation between several factors that have been implicated in the accessibility of transcriptional/translational regulatory elements and effectiveness of target sites of shRNA until now.

In the present study, we developed a promising tool for suppressing the expression of PPAR γ . Our PPAR γ -knockdown method will serve to clarify the role of the PPAR γ pathway in various cell types in vivo and in vitro, and will facilitate the development of therapeutic applications for a variety of diseases.

Acknowledgements: This work was supported in part by a grant (Tokuteiryouiki C13204072, to A.N.) from the Ministry of Education, Culture, Sports, Science and Technology, and a grant (15590227, to K.W.) from the Japan Society for the Promotion of Science.

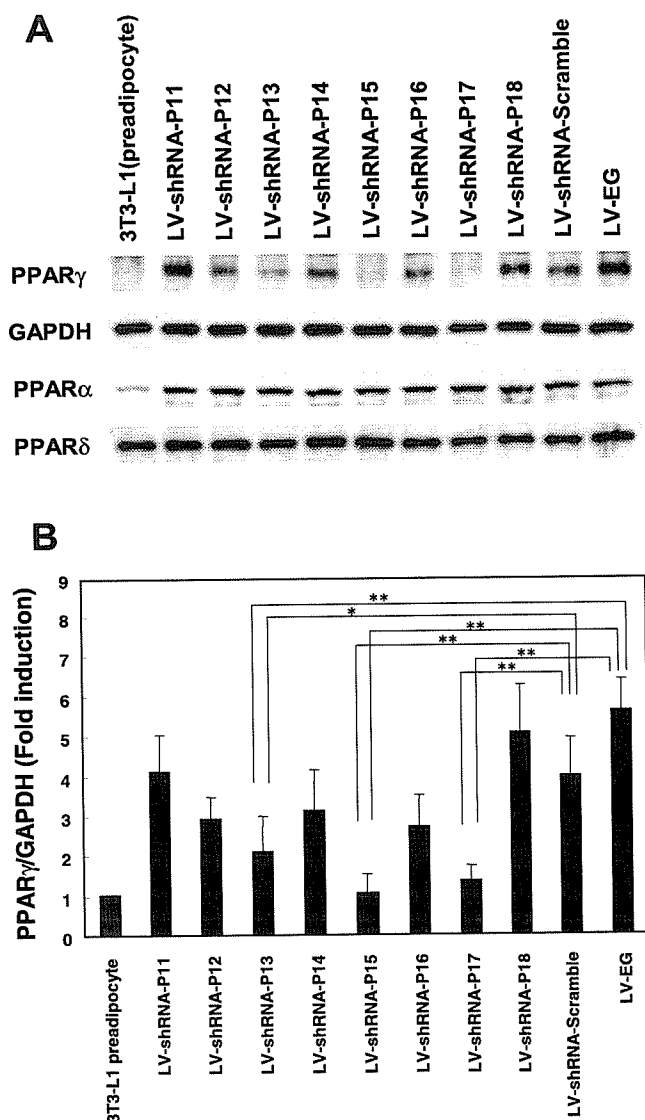


Fig. 4. Alteration of PPAR family protein levels in 3T3-L1 cells transduced with LV-shRNAs (200 MOI). A: Four days after the induction of adipocyte differentiation, the whole cell extract was analyzed by Western blotting with antibodies against PPAR γ , PPAR α , PPAR δ and GAPDH. Results are representative of three individual experiments. B: Densitometric quantitation for PPAR γ and GAPDH from three individual experiments. Each PPAR γ value was normalized over the basal level detected in 3T3-L1 preadipocytes (bars, S.E.M.). ** $P < 0.01$ for LV-shRNA-P13, -P15 and -P17 compared with LV-shRNA-Scramble or LV-EG. * $P < 0.05$ for LV-shRNA-P13 compared with LV-EG.